Environmental Science and Ecotechnology 20 (2024) 100368

Contents lists available at ScienceDirect

Environmental Science and Ecotechnology

journal homepage: www.journals.elsevier.com/environmental-science-and-ecotechnology/

Review

Enhancing photocatalytic CO_2 reduction with TiO_2-based materials: Strategies, mechanisms, challenges, and perspectives

Zhimin Yuan [a, 1], Xianglin Zhu [c, 1], Xianqiang Gao [f], Changhua An [d], Zheng Wang [b], Cheng Zuo [a], Dionysios D. Dionysiou [e], Hong He [b, *], Zaiyong Jiang [a, b, **]

[a] School of Chemistry & Chemical Engineering and Environmental Engineering, Weifang University, Weifang, 261061, PR China
[b] State Key Joint Laboratory of Environment Simulation and Pollution Control, Research Center for Eco-Environmental Sciences, Chinese Academy of Sciences, Beijing, 100085, PR China
[c] Institute for Energy Research, School of Chemistry and Chemical Engineering, Jiangsu University, Zhenjiang, 212013, PR China
[d] Tianjin Key Laboratory of Organic Solar Cells and Photochemical Conversion, School of Chemistry and Chemical Engineering, Tianjin University of Technology, Tianjin, 300384, PR China
[e] Environmental Engineering and Science Program, Department of Chemical and Environmental Engineering (DChEE), University of Cincinnati, Cincinnati, OH, 45221-0012, USA
[f] College of Forestry, Shandong Agricultural University, Taian, 271018, PR China

ARTICLE INFO

Article history:
Received 13 September 2023
Received in revised form
10 December 2023
Accepted 10 December 2023

ABSTRACT

The concentration of atmospheric CO_2 has exceeded 400 ppm, surpassing its natural variability and raising concerns about uncontrollable shifts in the carbon cycle, leading to significant climate and environmental impacts. A promising method to balance carbon levels and mitigate atmospheric CO_2 rise is through photocatalytic CO_2 reduction. Titanium dioxide (TiO_2), renowned for its affordability, stability, availability, and eco-friendliness, stands out as an exemplary catalyst in photocatalytic CO_2 reduction. Various strategies have been proposed to modify TiO_2 for photocatalytic CO_2 reduction and improve catalytic activity and product selectivity. However, few studies have systematically summarized these strategies and analyzed their advantages, disadvantages, and current progress. Here, we comprehensively review recent advancements in TiO_2 engineering, focusing on crystal engineering, interface design, and reactive site construction to enhance photocatalytic efficiency and product selectivity. We discuss how modifications in TiO_2's optical characteristics, carrier migration, and active site design have led to varied and selective CO_2 reduction products. These enhancements are thoroughly analyzed through experimental data and theoretical calculations. Additionally, we identify current challenges and suggest future research directions, emphasizing the role of TiO_2-based materials in understanding photocatalytic CO_2 reduction mechanisms and in designing effective catalysts. This review is expected to contribute to the global pursuit of carbon neutrality by providing foundational insights into the mechanisms of photocatalytic CO_2 reduction with TiO_2-based materials and guiding the development of efficient photocatalysts.

1. Introduction

Recent excessive consumption of fossil fuels has resulted in substantial dioxide (CO_2) emissions, leading to obvious climate warming and ecological and environmental challenges [1,2]. Controlling the ever-increasing CO_2 emissions has become an urgent problem. Inspired by photosynthesis in plants, the concept of artificial photosynthesis has emerged. This process involves photocatalytic CO_2 reduction into valuable fuels, such as carbon monoxide (CO), methanol (CH_3OH), methane (CH_4), and ethylene (C_2H_4), thereby aiming to reduce atmospheric CO_2 concentration. Therefore, the photocatalytic CO_2 reduction process garners substantial interest across science communities, governmental

* Corresponding author.
** Corresponding author. School of Chemistry & Chemical Engineering and Environmental Engineering, Weifang University, Weifang, 261061, PR China.
E-mail addresses: honghe@rcees.ac.cn (H. He), zaiyongjiang@qlu.edu.cn (Z. Jiang).
[1] These authors contribute equally to this work.

https://doi.org/10.1016/j.ese.2023.100368

agencies, and certain industries due to its cost-effectiveness and practicality [3–43].

Since 1978, when Halmann used gallium phosphide (GaP) semiconductor as a photoelectrode to reduce CO_2 to methanol and formic acid in H_2O solution [44], research in this area has attracted the interest of many researchers worldwide [45]. The reaction of photocatalytic CO_2 reduction only involves H_2O, CO_2 gas, solar light, and suitable photocatalysts, which is widely performed under mild conditions, i.e., low pressure and room temperature. In this process, the properties of the photocatalyst are crucial and can significantly affect the photocatalytic efficiency and the selectivity of the product. Therefore, in research efforts on the photocatalytic CO_2 process, exploring potential photocatalysts emerges as a critically significant area of focus. After decades of exploration, various effective photocatalysts for photocatalytic CO_2 reduction have been obtained, including TiO_2, bismuth oxychloride (BiOCl), carbon nitride (C_3N_4), bismuth vanadate ($BiVO_4$), GaP, bismuth tungstate (Bi_2WO_6), bismuth oxyiodide ($Bi_4O_5I_2$), high-entropy oxide $TiZrNbHfTaO_{11}$, high-entropy oxynitride $TiZrNbHfTaO_6N_3$, and metal-organic framework (MOF) [46–58]. Among them, TiO_2 is a promising candidate and has been widely studied due to its low cost, eco-friendliness, and easy synthesis [59]. Moreover, TiO_2 is confirmed to be very stable in the water solution environment and not sensitive to acid-base conditions, which is advantageous in photocatalytic CO_2 reduction processes. Its dependable catalytic performance has led it to be recognized as a reference material in the basic research process of photocatalytic CO_2 reduction. However, its band gap of 3.2 eV contributes to low solar energy utilization [60]. Meanwhile, it also endures poor separation efficiency of photogenerated electrons and holes, coupled with low CO_2 adsorption and activation capacity [61]. These limitations curtail its photocatalytic activity and product selectivity toward practical applications.

To overcome these difficulties in improving the catalytic activity and product selectivity of TiO_2, various modification strategies toward TiO_2 have been proposed, including element doping [62], surface plasmon resonance [63], heterojunction construction [64], control of crystal facets [65], built-in electric field [66], cocatalyst [67], morphological control [68], construction of oxygen vacancies [69], CO_2 adsorption tuning, and surface frustrated Lewis acid-base pair design [70,71].

Numerous studies have explored one or more strategies for modifying TiO_2 [72–75]. Low et al. [73] discussed the surface modification of TiO_2 for photocatalytic CO_2 reduction. Wang et al. [74] have focused on reviewing the defective TiO_2 (TiO_{2-x}) strategy for photocatalytic CO_2 reduction. Zhang et al. [76] focused on analyzing the strategies of visible light-sensitive TiO_2 photocatalysts. This review aims to provide a thorough examination of various TiO_2 modification strategies (Fig. 1) coupled with state-of-the-art analysis of pertinent strategies. Moreover, the review delves into the mechanisms underlying these modifications, elaborates on the current research challenges, and presents possible research directions in the future. This review is intended to serve as a reference for designing useful strategies to further advance the scientific knowledge and technological process in photocatalytic CO_2 reduction using TiO_2.

2. Mechanism of photocatalytic CO_2 reduction

The photocatalytic CO_2 progress based on the semiconductor photocatalysts involves generating electron-hole pairs and reducing CO_2 through photoelectrons. Meanwhile, the holes are consumed by H_2O or hole scavengers at the catalyst's surface. An efficient photocatalyst is characterized by an appropriate band structure, high carrier separation efficiency, and rich active sites. In experimental, the photocatalytic reaction mainly involves five consecutive steps (Fig. 2a) [75,77,78]:

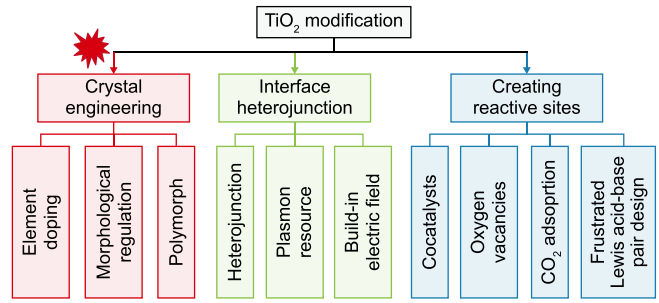

Fig. 1. The modification strategies of TiO_2 in this review.

(1) CO_2 adsorption on TiO_2 surface. The adsorption capacity will decide the surface reactant concentration, influencing the kinetic reaction rate. Appropriate adsorption energy can ensure the progress of the catalytic reaction and the smooth desorption of the product and regulate the selectivity of the CO_2 reduction reaction [8,79]. As a linear and nonpolar molecule, CO_2 has a tremendous energy of up to 750 kJ mol^{-1} to split the C=O bonds [80]. As a result, the activation of CO_2 molecules is the first huge barrier for the efficient photocatalytic CO_2 reduction reaction [81]. Unfortunately, the natural TiO_2 has insufficient adsorption capacity for CO_2, which seriously limits the final weak reduction efficiency. Until now, several approaches have been proposed to improve the CO_2 adsorption capacity of TiO_2, such as building vacancies and modifying cocatalysts. With these strategies, a

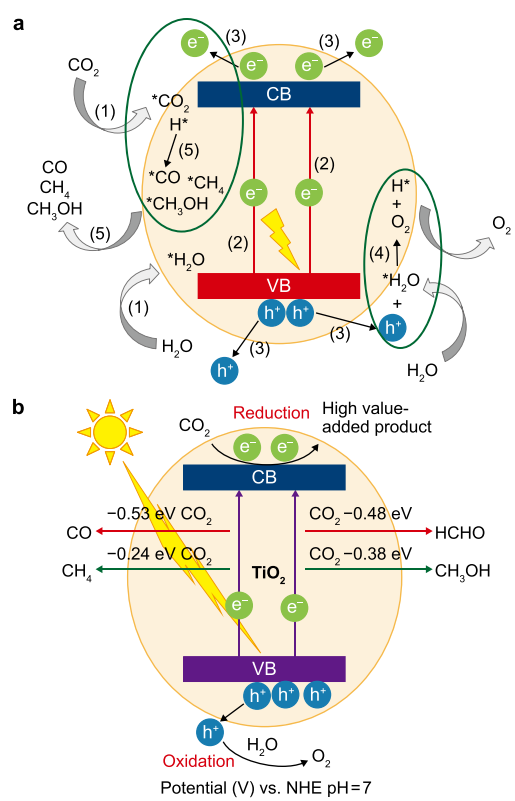

Fig. 2. a, Schematic of the mechanism of photocatalytic CO_2 reduction on TiO_2. **b**, Suitable reduction potential (vs. NHE at pH = 7) and corresponding products.

highly effective site will be constructed on the catalyst surface, which could interact with CO_2 molecules, forming CO_2* (active species with local charge). Accordingly, the linear structure becomes distorted and deformed, reducing the energy barrier of accepting photo-generated electrons [82].

(2) Under solar irradiation, TiO_2 becomes excited, generating photo-induced electron-hole pairs. TiO_2 has a band gap of 3.2 eV, indicating that it is primarily excited by UV light, which constitutes only 4.7% of the solar spectrum. To better exploit solar energy to produce more efficient photo-generated electrons, several modification measures are necessary to expand the light utilization range [83].

(3) Photo-generated electrons and holes migrate to the TiO_2 surface. Typically, only about 10% of the photogenerated carriers can move to the surface of TiO_2. Since the electrons and holes inside the crystal will recombine in 10 ns, such high recombination speeds limit the migration of many photo-generated carriers, resulting in a huge waste of light energy. Obviously, reducing the recombination efficiency of photogenerated carriers is critical to enhance photocatalytic CO_2 reduction activity. The improvement of the carrier separation was generally required both in the internal of the crystal and at the interface. For example, reasonable element doping or morphology regulation can achieve internal charge separation efficiency. As a result, the recombination of the electron-hole pairs will be inhibited by the formed intermediate energy levels or the nanostructure shortened migration distance. Besides, heterojunction construction and cocatalyst loading are widely used as efficient approaches to boost surface carrier separation [84–86].

(4) The photo-generated electrons on the TiO_2 surface reduce adsorbed CO_2 into CO, CH_4, CH_3OH, etc.; meanwhile, the holes are consumed by H_2O or scavengers. It is important to note that photo-generated electrons need suitable reduction potential to realize photocatalytic CO_2 reduction. Different potentials may correspond to different products; the theoretical data are given in Fig. 2b [87]. The conduction band potential of TiO_2 vs. normal hydrogen electrode (NHE) at pH = 7 is −0.5 V, which can reduce CO_2 into CH_4 and CH_3OH theoretically [88,89]. However, the vast majority of existing reports only confirmed the generation of CO [90–96], likely due to the suitable adsorption and activation of CO_2 or the change of pH, etc. In theory, photo-generated holes will oxidize H_2O into O_2, but the slow dynamic rate of H_2O oxidation also limits the final CO_2 reduction efficiency. The actual process of photocatalytic CO_2 reduction is still very complex, so the rate of product formation and product selectivity is influenced by many factors, including reduction potential, charge transfer, pH, TiO_2 surface environment, thermodynamics, kinetics, etc. [97,98].

(5) Product desorption from the TiO_2 surface. The reaction intermediates also play an important role in the CO_2 reduction process because their adsorption and desorption significantly affect the reaction activity and selectivity of products by controlling different reaction pathways. At present, the reaction process of photocatalytic CO_2 reduction using photocatalyst consists of three main pathways based on the reports of Saeid Akrami and Walsh et al. [53,99]: formaldehyde, carbene, and glyoxal pathways [99]. Based on the above-reported results, Wang et al. [100] proposed a detailed pathway display diagram (Fig. S1). These reaction pathways are guided via electron transfer, proton transfer (sometimes hydroxyl transfer), or concerted electron-proton transfer in photocatalytic CO_2 reduction. In general, these three main pathways proceed simultaneously. During the photocatalytic CO_2 reduction, a predominant reaction pathway is typically selected based on the collective conditions present during the experiment.

3. Promotion strategies of TiO_2 toward photocatalytic CO_2 reduction

Through nearly four decades of exploration, three main modification strategies of TiO_2 have been developed to improve its CO_2 reduction activity and product selectivity. This section presents a detailed discussion and summary of the latest advances and mechanisms of the aforementioned strategies.

3.1. Crystal engineering strategies

3.1.1. Element doping

The low utilization efficiency of solar light and photogenerated carriers are two crucial factors limiting the photocatalytic CO_2 reduction activity of TiO_2. Narrowing the band gap of TiO_2 is a useful approach to extend its light absorption capacity. Element doping has proven to be an effective strategy, facilitating the expansion of TiO_2's absorption spectrum into the visible range by reducing its band gap [101,102]. In addition, the induced impurity energy levels can also promote the charge separation capacity. According to the type of doped atom, we can divide elemental doping into non-metal doping and metal doping [103].

Recently, nitrogen (N), carbon (C), boron (B), sulfur (S), phosphorus (P), and iodine (I) can used as non-metal elements to enhance the activity of the TiO_2 through doping strategy. Adding a non-metal dopant results in forming an occupied state above the valence band of TiO_2 (Fig. 3a), thereby improving the utilization efficiency of solar light [104–109]. Wang et al. prepared a P-doped TiO_2 with enhanced activity toward the photocatalytic CO_2 reduction to CH_3OH, compared to that of pure TiO_2 (Fig. 3b) [105]. Experimental results proved that P^{5+} is doped into TiO_2 by substituting part of Ti^{4+} in TiO_2 to form the Ti-O-P bonds, thereby reducing the band gap of TiO_2 to 3.02–3.12 eV, depending on different P doping contents (Fig. 3c). The absorption region of P-

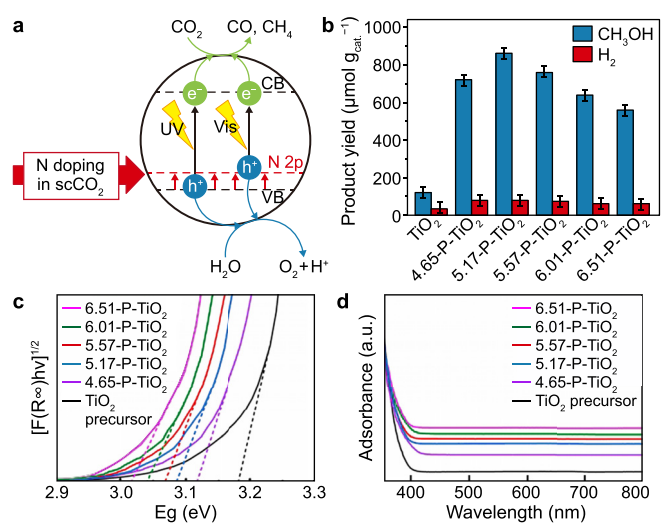

Fig. 3. **a**, The occupied state diagram above the valence band of TiO_2 [104]. **b**, Photocatalytic methanol generation via TiO_2 and P-TiO_2 samples. **c**, Plots of $(ahv)^{1/2}$ versus the photon energy (hv). **d**, Absorption spectra of the P-TiO_2 samples. Adapted with permission from Ref. [104]. Copyright 2022, Multidisciplinary Digital Publishing Institute. Adapted with permission from Ref. [105]. Copyright 2016, Elsevier B.V.

doped TiO_2 was obviously extended to the visible light (Fig. 3d). In addition, the formed new occupied state above the valence band derived from the doping of P element serves as electron acceptor centers, exhibiting lower recombination rate of photo-generated carriers. The above two factors are responsible for the improvement of catalytic performance. Besides, Bjelajac et al. [110] synthesized N-doped TiO_2 nanoparticles, and the successful doping of N extends the light absorption region (Figs. S2a–b), restraining the fast recombination of electron and hole pairs. These two factors resulted in N-doped TiO_2 with significantly improved photocatalytic CO_2 reduction activity compared to the pristine sample (Fig. S2c).

In addition, Zhang et al. have investigated I-doped TiO_2, which was synthesized via a hydrothermal strategy [103]. It was found that I^{5+} replaced Ti^{4+} to form I-O-Ti bands because of their similar ionic radius, thereby making the doped TiO_2 yellow. Moreover, I-TiO_2 catalysts exhibited an obviously enhanced light absorption, with their band gaps gradually decreasing with the increasing amount of I doping (Figs. S3a–b). In addition, doping could facilitate the separation of photo-generated carriers. Therefore, all I-TiO_2 samples exhibited higher CO_2 reduction activities than pure TiO_2 (Figs. S3c–d). But 5% iodine doping sample showed the best activity, indicating that high doping concentration could enhance the number of charge recombination centers that inhibit the effective separation of photo-generated electrons and holes. Recently, Amin et al. reported a series of carbon-doped TiO_2 samples (3D structure images are shown in Figs. S4a–b) and systematically investigated their photocatalytic CO_2 reduction activities [111]. The introduction of carbon into TiO_2 caused the narrowing of its band gap and made it possess significant visible light absorption (Fig. S4c). Moreover, carbon doping is important in affecting photo-generated carriers' recombination. In their studies, 4.5C- and 7.5C-TiO_2 samples exhibited similar CO_2 reduction activity to TiO_2 (Fig. S4d); however, 6C-TiO_2 showed an obvious performance enhancement compared to other catalyst tests. This work indicated that a low doping amount cannot provide enough active sites and significantly reduces the rapid recombination of electrons and hole pairs. On the other hand, excessive carbon doping harms separating photo-generated carriers due to the formation of charge recombination centers. In conclusion, optimizing the doping concentration of non-metals in TiO_2 is crucial for the maximum possible enhancement of photocatalytic CO_2 reduction activity.

Metal doping was also proven an efficient tactic to expand the solar light utilization of TiO_2 via introducing the defect level below the conduction band (CB) of TiO_2 (Fig. S5a) [112–114]. Furthermore, the photo-generated electrons can also flow from the CB of TiO_2 to the defect level, thereby realizing the effective separation of photon-generated carriers. Both aspects are very beneficial for the photocatalytic CO_2 reduction of TiO_2. Recently, metal elements, including iron (Fe), copper (Cu), cobalt (Co), nickel (Ni), manganese (Mn), molybdenum (Mo), vanadium (V), europium (Eu), magnesium (Mg), and indium (In), have been used to engineer the properties of TiO_2 [114–120]. Liu et al. prepared Fe-doped TiO_2 octahedra using hydrothermal and calcination methods (Fig. S5b) [119]. Fe^{3+} ions were uniformly doped into TiO_2 lattice because of the similar ion radius of similar size. The Fe doping produced a dopant energy level below the CB of TiO_2 (Fig. S5c), thus promoting the effective space separation of photogenerated electrons and holes and narrowing the band gap of TiO_2 to 2.42 eV (Figs. S5d–e). The reduced band gap enables TiO_2 to absorb more solar light to participate in the photocatalytic CO_2 reaction. Therefore, Fe-doped TiO_2 exhibited a much higher CH_4 yield than pure TiO_2 (Figs. S5f–g).

Besides, Feng et al. obtained a series of Mo-TiO_2 samples using the hydrothermal method [120]. It was proven that the absorption capacity of Mo-TiO_2 in visible light field gradually increased with the doping amount of Mo increasing (Fig. 4a). In addition, the results of photocurrent (Fig. 4b), fluorescence spectra (Fig. 4c) and electrochemical impedance spectroscopy (Fig. 4d) supported the conclusion that the efficiency of photo-generated charge-carrier separation of Mo-TiO_2 was higher than that of pure TiO_2. In addition, it was confirmed that the doping of Mo could activate H_2O molecules, thereby providing more protons to reduce CO_2. These advantages enabled the Mo-TiO_2 sample to improve the photocatalytic CO_2 reduction into CH_4 (Fig. 4e and f).

3.1.2. TiO_2 polymorph

In general, the light absorption activity of semiconductor photocatalysts is strongly influenced by their crystal structure. There are three main phases of TiO_2 under air pressure: brookite (bandgap: ca. 3.3 eV), anatase (bandgap: ca. 3.2 eV), and rutile (bandgap: ca. 3.0 eV). For the past few years, the three TiO_2 polymorphs have been widely explored and studied in photocatalytic CO_2 reduction and have made great progress [121]. However, the light absorption capacities of the three TiO_2 polymorphs are all limited to the ultraviolet light range. Recently, the dopant-free method in the pristine TiO_2 crystal also become a research spotlight to extend its light absorption capacity [122]. The high-pressure phases of TiO_2 have been confirmed to exhibit small bandgaps via theoretical research [123]. For instance, Hadi Razavi-Khosroshahi et al. [124] reported the bandgap of the nanosized TiO_2-II (columbite) phase is ca. 2.4 eV. Wang et al. [125] found the TiO_2-II polymorph formed via high-pressure torsion processing exhibited excellent photocurrent performance under visible light. A conclusion can be drawn: designing TiO_2 polymorphs to expand the light absorption capacity of titanium dioxide is a good modification

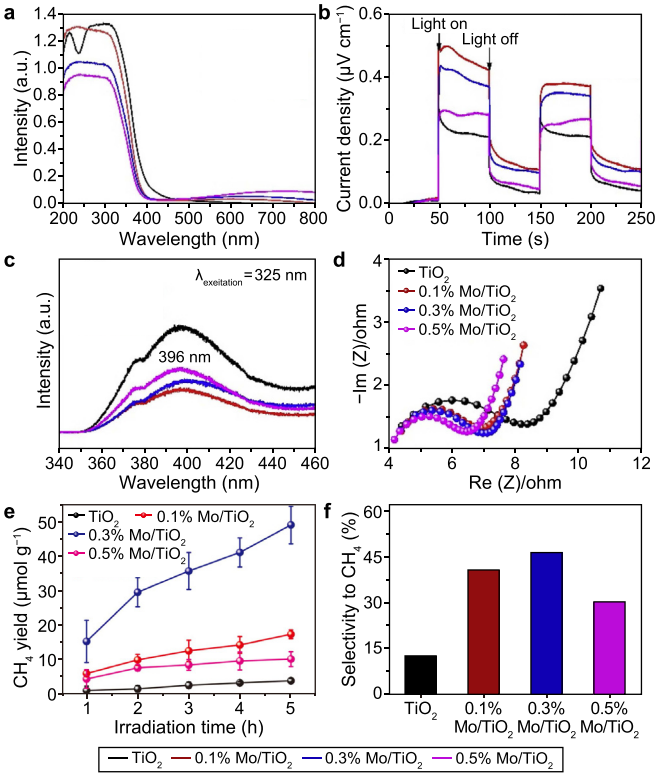

Fig. 4. UV-vis absorption spectra (**a**), photocurrent (**b**), fluorescence spectra (**c**), electrochemical impedance spectroscopy (**d**), CH_4 yield (**e**), and CH_4 selectivity (**f**) of TiO_2 and Mo-TiO_2 samples. Adapted with permission from Ref. [120] Copyright 2020, Elsevier B.V.

strategy for photocatalytic CO_2 reduction applications.

Saeid Akrami et al. [126] prepared the TiO_2-II polymorph vis using a high-pressure technique (HPT) to process the initial anatase TiO_2. Their light absorbance result has proved the TiO_2-II polymorph has a low bandgap, ca. 2.5 eV. Photocurrent tests exhibited that the current density for initial anatase TiO_2 is smaller compared to that of the TiO_2-II polymorph. The TiO_2-II polymorph enhances photocatalytic CO_2 into CO than pristine anatase TiO_2. This expanded light absorption should be important in improving the above activity.

3.1.3. Morphological regulation

Morphology regulation is another potential method to enhance the photocatalytic CO_2 reduction activity over TiO_2 [127]. The common morphologies of TiO_2 include nanoparticles, nanosheets, microspheres, nanowires, nanoflower, nanorods, mesoporous materials, nanotubes, hollow structures, etc. [128–133]. The transformation of TiO_2 morphologies can result in different characteristics, such as surface area, crystallinity, size dimension, porosity, and concentration of active site concentration, which in turn influence the CO_2 activation, the photon adsorption, the separation efficiency of photo-generated electrons and holes, and the desorption of intermediates, and so on [132–135]. Overall, the transformation of TiO_2 morphologies can result in significantly different photocatalytic CO_2 reduction activity.

Fu et al. [68] synthesized mesoporous TiO_2 nanofibers via electrospinning. As shown in Fig. S6, the diameter of the nanofiber is about 300 nm, and all nanofibers exhibited mesoporous structures made of interlaced nanocrystals of ca. 10 nm. The special structure makes TiO_2 possess large specific surface areas; meanwhile, enough -OH groups exist on the surface of TiO_2. These factors enable TiO_2 to separate photo-generated charge carriers effectively and improve CO_2 adsorption capacity, leading to excellent photocatalytic CO_2 reduction. Di et al. [134] prepared porous TiO_2 (B) with hierarchical nanostructure composed via ultrathin nanosheets. The structure possessed a high surface area and offered abundant CO_2 adsorption active sites, enabling it to exhibit outstanding photocatalytic CO_2 reduction to CH_4 and CH_3OH. Koci et al. [135] prepared 4.5–29 nm sized TiO_2 particles and studied their photocatalytic CO_2 reduction tests. The results showed that 14 nm-sized TiO_2 particles possessed the best performance, which could be attributed to the competing effects of charge carrier dynamics, surface area, and light adsorption efficiency.

According to the principle of crystallography, the exposed facets of the catalyst are pivotal for the catalytic reactions. The kind of exposed atoms and active sites can be achieved by facets engineering. The energy barrier difference between the crystal facets can also facilitate the separation of charge carriers. In general, anatase TiO_2 photocatalyst tends to expose (101) facets because it has low energy (0.44 J m^{-12}) compared to that of (001) facets (0.90 J m^{-12}) [65,136]. As an outstanding surface photocatalyst, pentacoordinate Ti (Ti_{5c}) on the facets is a highly active site toward photocatalytic CO_2 reduction (Figs. S7a–c). However, the commonly exposed (101) facets only have 50% Ti_{5c} [65], which is insufficient for photocatalytic CO_2 reduction, thus possibly limiting the catalytic activity. It has been confirmed via the DFT (Density Functional Theory) electronic structure calculations that the surface heterojunction could form between the (001) and (101) facets (Figs. S7d–e) [136]. The light proportions and the transfer and separation efficiencies of photo-generated charge carriers would be improved by adjusting the exposed facets, which is helpful to enhance the photocatalytic CO_2 reduction of TiO_2 [137,138]. Therefore, controlling the crystal facets of TiO_2 crystal is an important strategy to promote its CO_2 reduction activity.

Jiang et al. produced TiO_2 (100) facets via a Zeeman-effect-assisted anodic oxidation way, which contained lower coordinated Ti atoms [65]. It exhibited high photocatalytic CO_2 reduction into ethanol, 22 times higher in yield than pure TiO_2. *In situ* Fourier transforms infrared spectroscopy (FTIR) and DFT calculations both revealed the low coordinated Ti atoms at the (100) facets are helpful to couple CO* intermediates adsorption. In addition, the exposure ratio of (100) facets was up to 48.01%, and the remaining were (101) and (001) facets. As mentioned, the facets heterojunction resulted in a more effective migration of photo-generated charge carriers in the CO_2 reduction reaction. These factors are responsible for the improvement of converting CO_2 to ethanol. Recently, platinum (Pt) single atoms (SAs) and Ni nanoclusters (NCs) have been introduced onto the (001) facet, and a small amount of Ni clusters were deposited on the (101) facet of hydrogenated TiO_2 nanosheets by a room temperature H_2/Ar (argon) plasma method. The H-O bond of the adsorbed H_2O molecule was significantly activated on the Pt SAs-TiO_2 and Ni NCs-TiO_2. This work provides a new opportunity to design advanced crystal facet-induced engineering nano-catalysts [139].

3.2. Design of interface heterojunction catalyst

3.2.1. Construction of semiconductor/semiconductor heterojunction

Combining TiO_2 with another semiconductor can form a composite catalyst with excellent contact called TiO_2 heterojunction. Based on the type of the combined semiconductor, the traditional heterojunction could be divided into two categories: n-n heterojunction and p-n heterojunction. Recently, the new Z-scheme heterojunction photocatalysts have been proposed, and many of these materials demonstrated excellent performances. In photocatalytic CO_2 reduction using TiO_2 heterojunction, the heterojunction could significantly facilitate the effective separation of photo-generated electrons and holes, resulting in good photocatalytic activity [140–152].

In general, the TiO_2-based n-n heterojunction has three types of band alignments, including the straddling gap (Fig. 5a), staggered gap (Fig. 5b), and broken gap (Fig. 5c) [153]. As shown in Fig. 5a, the electrons and holes simultaneously assemble at CB and VB of B semiconductors, not realizing their effective separation. It can be observed that the electrons and holes could not transfer between A and B semiconductors due to the broken gap (Fig. 5c). However, the staggered gap (Fig. 5b) could enable electrons to accumulate at CB of B semiconductor and holes to accumulate at VB of A semiconductor, thereby achieving effective spatial separation. Therefore, the staggered gap, also usually named type-II heterojunction, was widely studied in the process of photocatalytic CO_2 reduction.

Kim et al. [154] synthesized the $TiO_2/ZnIn_2S_4$ composite as a type-II heterojunction via simple hydrothermal and impregnation methods (Fig. S8), named TNT-ZIS. Subsequently, the photocatalytic CO_2 reduction of all samples was performed using $Co(bpy)_3^{2+}$ as catalytic active centers and triethanolamine (TEOA) as the electron donor. As shown in Fig. 6a, the TNT-ZIS sample improved performance compared to bare TiO_2 and $ZnIn_2S_4$. Moreover, it can be observed in Fig. 6b that TNT-ZIS possessed excellent stability in the process of CO_2 reduction. In Fig. 6c, TNT-ZIS heterojunction exhibited an obvious strong photocurrent and relatively weak electrochemical impedance compared to pure TiO_2 and $ZnIn_2S_4$, indicating a more effective separation of photo-generated electrons and holes. Fig. 6d shows the schematic mechanism of the TNT-ZIS composite toward photocatalytic CO_2 reduction. In the reaction process, the generated electrons accumulated at CB of TiO_2, and holes left or flowed to VB of ZIS, separating the photo-generated charge carriers and enhancing the photocatalytic activities.

The formed heterojunction that combines the p-type semiconductor with TiO_2 is called TiO_2-based p-n heterojunction. After

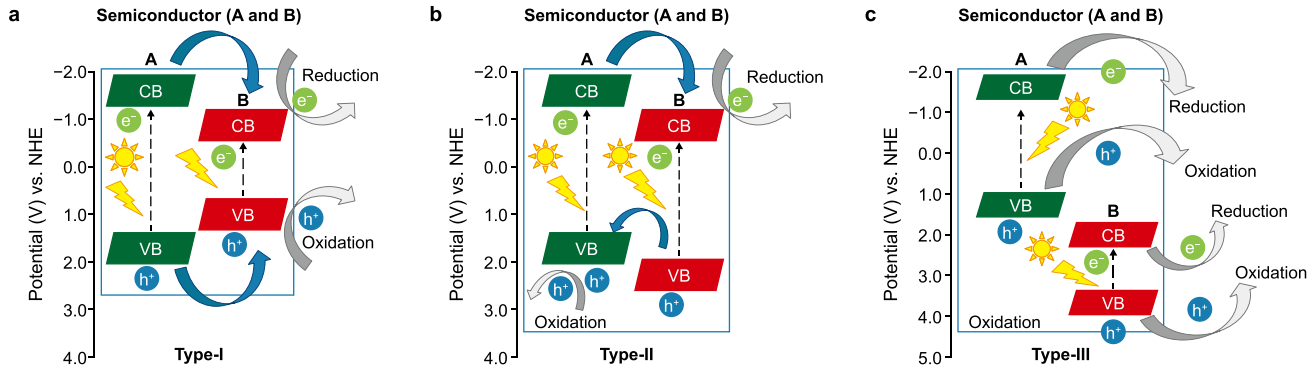

Fig. 5. Three types of band alignments for n-n heterojunction: **a**, straddling gap (Type-I); **b**, staggered gap (Type-II); **c**, broken gap (Type-III).

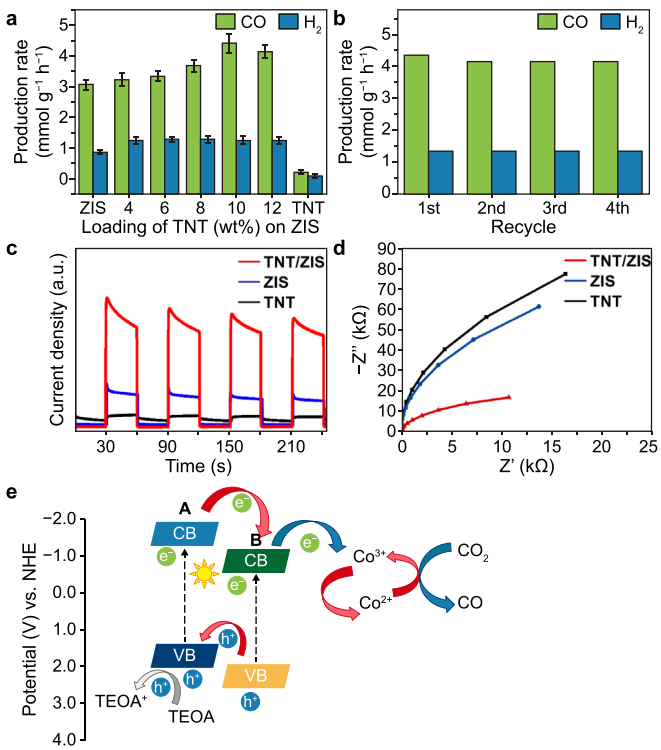

Fig. 6. **a**, Photocatalytic CO_2 reduction activities of all samples. **b**, Repeated experiments of $TiO_2/ZnIn_2S_4$-10. **c**, Photocurrent and electrochemical impedance spectra. **d**, Mechanism illustration of CO_2 reduction of $TiO_2/ZnIn_2S_4$. Adapted with permission from Ref. [154]. Copyright 2022, Elsevier B.V.

forming p-n heterojunction, an electric field will be produced between TiO_2 and p-type semiconductor due to their disparity of Fermi level, accelerating the separation of charge carriers more effectively [155–157]. For instance, Yang et al. [155] fabricated the TiO_2/Cu_2O (cuprous oxide) p-n heterojunction via a simple chemical reduction procedure. Compared to pure TiO_2 and Cu_2O, the TiO_2/Cu_2O composites exhibited an enhanced photocatalytic CO_2 reduction activity performance (Figs. S9a–b). In addition, the photocurrent and electrochemical impedance properties have been tested to discover the separation of charge carriers' capacities. As shown in Fig. S9c, the TiO_2/Cu_2O-15% showed better photoelectric activity than pure TiO_2 and Cu_2O. Moreover, it can be observed that the TiO_2/Cu_2O-15% sample exhibited the smallest electrochemical impedance (Fig. S9d). The results indicated that forming p-n heterojunction could improve the separation of electron-hole pairs and boost the rapid charge migration. Based on the proposed possible mechanism in Fig. S10, under solar light irradiation, TiO_2 and Cu_2O are induced to generate electrons and holes, which will accumulate at CB of TiO_2 and VB of Cu_2O under the function of the internal electric field, respectively. The internal electric field induces a more efficient charge separation. Therefore, the photocatalytic CO_2 reduction activities of TiO_2/Cu_2O were enhanced.

Although the TiO_2-based Z-scheme heterojunction has a similar band structure to the aforementioned two kinds of heterojunction, the photo-induced electrons and holes exhibit a different transmission path [158–160]. In the Z-scheme heterojunction, the photo-generated electrons of TiO_2 will recombine with the holes derived from the coupled photocatalyst [161,162]. Subsequently, the holes at VB (valence band) of TiO_2, possessing a much stronger oxidation capacity than that of coupled photocatalysts, would be maintained. On the other hand, the photo-generated electrons with a stronger reduction capacity are kept on the CB (conduction band) of the coupled photocatalyst. Therefore, Z-scheme heterojunction could not only inhibit the recombination of photo-generated electron-hole pairs but also take full advantage of the strongest redox capacities of the composite photocatalyst. These advantages will promote the photocatalytic CO_2 reduction activity of TiO_2 [163].

Tahir et al. [164] prepared a (zinc ferrite) $ZnFe_2O_4/TiO_2$ Z-scheme heterojunction via a facile hydrothermal method. It was found that the $ZnFe_2O_4/TiO_2$ composite exhibited a significantly improved photocatalytic CO_2 reduction to CO (Fig. S11a). The PL spectra analysis was performed to study the recombination of photo-generated electrons and hole pairs in pure TiO_2 and $ZnFe_2O_4/TiO_2$ composite. The $ZnFe_2O_4/TiO_2$ showed a much lower PL intensity under 325 nm excitation wavelength than pure TiO_2, indicating an effective charge separation between TiO_2 and $ZnFe_2O_4$ [164]. A Z-scheme heterojunction mechanism was proposed in Fig. S11b. The CB and VB positions of $ZnFe_2O_4$ are about −1.36 and 0.63 eV, respectively. Its VB position keeps a proper distance from the CB of TiO_2 (−0.5 eV), resulting in the CB electrons of TiO_2 transferring toward the VB of $ZnFe_2O_4$ to recombine with its holes. Finally, holes with stronger oxidation capacity and electrons with stronger reduction capacity would be effectively separated. The CB electrons of $ZnFe_2O_4$ will reduce CO_2 into CO, and the holes at VB of TiO_2 will oxidize the H_2O molecule to produce H^+ to meet the need for CO_2 reduction. In addition, when a metal (e.g., Ag nanoparticle) is introduced between TiO_2 and $ZnFe_2O_4$ heterojunction, the electrons transfer from CB of TiO_2 to VB of $ZnFe_2O_4$ is promoted (Fig. S11c). The functionality of the Z-scheme heterojunction is significantly enhanced, confirmed via PL spectra and photocatalytic CO_2 reduction of $ZnFe_2O_4$/Ag (silver)/TiO_2.

3.2.2. Surface plasmon resonance enhancement strategies

Recently, plasmonic metals, such as Ag, Au (gold), and Cu, with a strong special SPR effect, are generally used to modify TiO_2 to boost its photocatalytic CO_2 reduction of TiO_2 [165–173]. Each plasmonic metal has its unique oscillation frequency of free electrons. In the process of photocatalytic CO_2 reduction, if the energy of incident light is consistent with the frequency, this light will induce the surface plasmon resonance (SPR) effect to generate a localized electromagnetic field and hot electrons on the surface of metals (Fig. S12a) [63,174–177]. These hot electrons could transfer to the conduction band of neighboring TiO_2 to improve the surface electron density, enhancing the photocatalytic CO_2 reduction activity of TiO_2. In addition, due to the difference in Fermi level between the plasmonic metal and TiO_2, the photo-generated electrons derived from the conduction band of TiO_2 will transfer to plasmonic metals to realize the Fermi equilibrium of the composite materials (Figs. S12b–c), achieving effective separation of photo-generated charge-carrier. The above two causes are responsible for improving TiO_2 activity via the SPR effect.

Tahir et al. [178] prepared an Ag/TiO_2 composite in which Ag nanoparticles were uniformly distributed on the surface of TiO_2. Large- and small-size Ag nanoparticles with similar content coexisted in the sample. The absorption spectra showed that an obvious plasmon response located between 470 and 670 nm was generated due to the load of Ag (Fig. S13a), which significantly improved the light absorption capacity of TiO_2. Under the irradiation of visible light, hot electrons will be excited by the large-size Ag particles due to the localized SPR and then migrate to the surface of TiO_2. Subsequently, these electrons are trapped by the small-size Ag (Fig. S13b). The above process gives Ag/TiO_2 the capacity to achieve a more efficient photocatalytic CO_2 reduction under visible light than pure TiO_2. Additionally, under UV light irradiation, TiO_2 is excited and produces photo-generated electrons that flow into the CB of TiO_2. These electrons are captured by Ag, thereby achieving the effective spatial separation of photo-generated charge carriers. The photocatalytic CO_2 reduction activity of Ag/TiO_2 is thus significantly improved (Figs. S13c–d).

3.2.3. Surface built-in electric field construction

In photocatalytic CO_2 reduction over TiO_2, the separation efficiency of photo-generated electrons and holes is crucial for the final reaction efficiency. Recently, constructing a built-in electric field using the different properties of semiconductor photocatalysts has been considered an excellent method to efficiently separate photogenerated electrons and holes [11,179]. This efficiency is attributed to the migration of electrons and holes in opposite directions, driven by the electric field at the interface [180,181]. Therefore, it is reasonable to enhance its photocatalytic CO_2 reduction activity by modifying the built-in polar field on the TiO_2 surface [182].

Li et al. [66] designed the Bi (bismuth) ions-modified TiO_2 nanosheets via an ionic adsorption strategy. DFT calculations demonstrated that the electrons of Bi transfer onto TiO_2 through the connection between TiO_2 and the absorbed Bi ions, which could induce a built-in electric field from the surface to the interior of the TiO_2 substrate. Subsequently, the surface photovoltage (SPV) and PL (photoluminescence spectroscopy) spectra measurements were performed to confirm that the separation capacity of the photogenerated charge carrier could be effectively increased after introducing Bi ions. As a result, the TiO_2-Bi sample exhibited a significant enhancement of photocatalytic CO_2 reduction compared to pure TiO_2. Therefore, the design of a built-in electric field is very feasible to facilitate fast charge transfer and effective separation, further improving the photocatalytic CO_2 reduction of TiO_2.

3.3. Creating reactive sites

3.3.1. Cocatalysts modification

Recently, many researchers have proven that the loading of cocatalysts on the surface of TiO_2 could significantly improve photocatalytic CO_2 reduction activity and selectivity [183–185]. In the whole catalytic process, the cocatalysts could influence several reaction factors: (1) decreasing CO_2 activation energy and reaction overpotential; (2) accelerating the effective separation of photogenerated electrons and holes; (3) tuning the activation and adsorption of different intermediates; (4) inhibiting the side reactions (such as H_2 evolution reaction) [186,187]. Up to now, many cocatalysts have been found and applied in the photocatalytic CO_2 reduction of TiO_2, for example, noble metals (i.e., Ag, Pt, palladium (Pd), ruthenium (Ru)), non-noble metals (i.e., Cu, Ni), and other some materials (such as graphene, chromic oxide (Cr_2O_3), molybdenum sulfide (MoS_2), Tri-nickel boride (Ni_3B)) [188–196].

Zhang et al. [197] deposited Pt nanoparticles onto the surface of TiO_2 to obtain a series of Pt/TiO_2 samples. Subsequently, their photocatalytic CO_2 reduction reactions were tested, and the results are shown in Fig. S14a. It could be seen that the load of Pt significantly improved the photocatalytic activities of TiO_2. The 0.12 wt% Pt loading amount on TiO_2 has exhibited the best performance toward the CH_4 product. The further enhancement of the loading amount is likely to result in the covering of the active sites and the hindering of the solar light absorption (resulting in a reduction of the number of photo-generated charge carriers) [187]. A feasible photocatalytic mechanism was proposed and shown in Fig. S14b. Under UV light irradiation, TiO_2 is excited to generate electrons, which are subsequently transferred to the CB of TiO_2. Because the work function of Pt is higher than that of TiO_2, the photo-generated electrons continued to migrate to the Pt surface, further prompting the effective separation of charge carriers. Therefore, the loading of Pt cocatalyst significantly improved the photocatalytic CO_2 reduction of TiO_2.

The inherent costliness and limited availability of noble metals generally pose significant challenges to their extensive application in photocatalytic CO_2 reduction on a large scale. Therefore, non-noble metals (i.e., Cu, Ni) cocatalysts have attracted increasing attention and have been widely studied [198–200]. For example, our group has synthesized a series of Cu/TiO_2 by an *in situ* online synchronous photo-deposition method [198]. Fig. S14c shows the Cu element was atomically dispersed on the surface of TiO_2 nanosheets. Subsequently, the photocatalytic CO_2 reduction experiments were performed, and the results are shown in Fig. S14d. It can be found that the introduction of the Cu element improved CO yield after 2 h of light irradiation compared to that of pure TiO_2. Similar to the above-mentioned Pt excess load, a further increase in Cu loading resulted in a decreased CO_2 conversion rate. Similarly, the non-noble metal Cu cocatalyst enhances the photocatalytic CO_2 reduction of TiO_2 by facilitating the effective separation of photogenerated electrons and holes.

During the progress in the field of photocatalytic CO_2 reduction, researchers realized that the improvements using a single cocatalyst to enhance the activity and selectivity of TiO_2 in photocatalytic CO_2 conversion, the efficiency was still insufficient to meet the real demand. Based on this point, the alloy cocatalysts or bimetal cocatalysts have been considered a novel strategy for further improving the performance of TiO_2 [201–206]. Wei et al. [207] constructed Pt-Ru alloy on the surface of TiO_2 by a simple photon-assisted method. The EDS elemental mapping in Fig. 7a indicated a similar dispersion of Pt (light blue) and Ru (dark blue) in the sample. Moreover, the Pt nanoparticles help accelerate the stripping of H atoms from H_2O and accumulate the surface photogenerated electrons, exhibiting relatively high selectivity for CH_4.

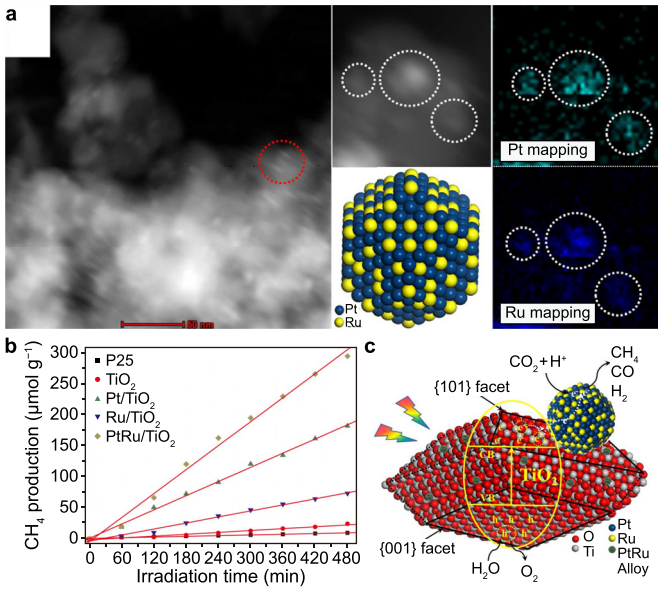

Fig. 7. **a**, EDS mapping of PtRu/TiO_2. **b**, Photocatalytic CO_2 reduction to CH_4 rates of samples. **c**, Schematic illustration of photocatalytic CO_2 reduction via PtRu/TiO_2. Adapted with permission from Ref. [207]. Copyright 2018, Elsevier B.V.

The Ru nanoparticles showed strong adsorption/activation capabilities for CO_2; thus, Ru/TiO_2 mainly produced CO gas during CO_2 reduction. Moreover, coupling Pt with Ru together as an alloy cocatalyst on the surface of TiO_2 could effectively exert a synergistic effect. So, among these samples, the PtRu/TiO_2 exhibited the best activity in photocatalytic CO_2 reduction into CH_4 (Fig. 7b). The relevant mechanism was proposed and is shown in Fig. 7c. In the process of photocatalytic CO_2 reduction, photo-generated-electrons derived from TiO_2 migrated to PtRu alloy to spatially separate the charge carrier and reduce CO_2. Meanwhile, the Ru component in alloy plays an important role in CO_2 adsorption and activation, and Pt constituently enriches H species from the oxidation of H_2O. Finally, under the synergic effect of Ru and Pt, the modified TiO_2 exhibits a high reaction rate and selectivity of CH_4.

Although metal cocatalysts have many advantages for improving the photocatalytic CO_2 reduction of TiO_2, pristine metal cocatalysts also have some intractable problems. For instance, many metals have too strong adsorption effects for CO, which will impede further transformation of CO_2, even though excessive CO accumulation may lead to partial deactivation of catalysts [193]. In addition, the strong adsorption effect for some intermediates increases the difficulty of changing the selectivity of the reaction product. Therefore, researchers have begun to explore other materials, such as graphene, Cr_2O_3, MoS_2, and Ni_3B, when conducting in-depth research on metal cocatalysts [182,193,195]. Zhou et al. [193] loaded Ni_3B on the surface of TiO_2, in which the Schottky junction is formed between TiO_2 and Ni_3B because of the low Fermi energy level of Ni_3B, making the photo-generated electrons of TiO_2 transfer to Ni_3B. The p-states of B atoms and d-states of Ni could induce strong hybridization to form new d-band centers. This could activate the adsorbed CO_2 on the catalyst's surface and induce a continuous protonation effect to produce deep hydrocarbons. Therefore, Ni_3B on the surface of TiO_2 could be used as a co-catalyst to improve the generation rate and selectivity of CH_4.

3.3.2. Oxygen vacancies construction

Constructing oxygen vacancies in TiO_2 crystals could adjust their electronic structures, enhance the surface-active sites, tune the adsorption capacity for gas oxides, and modulate the band gap, influencing their photocatalytic activity [74]. Due to the absence of oxygen atoms in the crystal of TiO_2, the obtained oxygen vacancy sites could serve as the center of a negative charge, meanwhile generating an oxygen defect level between the CB and VB of TiO_2 (Fig. S15) to reduce its band gap [208]. It enables TiO_2 to absorb visible light to expand the utilization of solar light, and a reasonable concentration of oxygen vacancies can even extend light absorption of TiO_2 to the near-infrared region [74,209]. In addition, defect levels could accumulate the photo-generated electrons on the CB, facilitating the effective separation of electrons and holes. Some research studies have confirmed that surface oxygen vacancy could improve the CO_2 adsorption capacity and bend the linear CO_2 molecule via the bonding of oxygen atoms of CO_2, reducing the reaction barrier for the breakage of the C-O band [210]. Based on these advantages, constructing oxygen vacancies in TiO_2 crystal is expected to become a promising method to enhance the photocatalytic CO_2 reduction activity [211–216].

Deng et al. [217] prepared TiO_{2-x} nanostructures via a simple hydrothermal strategy. They found that all TiO_{2-x} samples exhibited an obvious visible light absorption between 400 and 600 nm. As the oxygen vacancy concentration increases, the band gap of TiO_{2-x} gradually decreases; meanwhile, the redox capacity also decreases gradually. The photocatalytic CO_2 reduction study of the samples indicated the TiO_{2-x}-24 h sample possessed the highest catalytic activity. Excessive oxygen vacancies resulted in the formation of electron recombination centers, leading to decreased performance because of the weakened redox capacity. In this paper, they proposed a possible mechanism for improved photocatalytic CO_2 reduction. The oxygen vacancies in TiO_{2-x} improved the chemical adsorption of CO_2 and activated CO_2 to generate $*CO_2^-$ species. Under the light irradiation, photo-generated electrons derived from TiO_2 reduced $*CO_2^-$ to CH_4. Meanwhile, the photo-generated charge carriers were effectively separated due to oxygen vacancies at proper concentration. In addition, the narrowed band gap extended the light absorption region of TiO_2, thereby enabling TiO_{2-x} to exhibit visible light activity [218].

3.3.3. CO_2 adsorption capacity enhancement

As is well-known, reducing a linear CO_2 molecule to $CO_2^{\bullet-}$ via a single electron needs a very high reduction potential, ca. −1.90 V vs. NHE [218]. It is very hard for TiO_2 to transform the linear CO_2 molecule directly into high-value-added organic products. To reduce the high energy demand, the structure reorganization of CO_2 molecules is necessary. Fortunately, the function of CO_2 surface adsorption on TiO_2 can distort the linear structure to generate bent $*CO_2$ species [219,220], significantly decreasing the catalytic reduction potential. Therefore, in photocatalytic CO_2 reduction on the TiO_2, CO_2 adsorption is a crucial factor [221]. Recently, researchers developed several methods to improve the CO_2 adsorption properties of TiO_2, mainly consisting of increasing specific surface area, compositing activated carbon with high CO_2 adsorption capacity, modifying Lewis base on its surface, etc. [222].

The construction of hollow structures represents a clear strategy to realize efficient photocatalysts with a high specific surface area. Lee et al. prepared TiO_2 hollow spheres (TOH) with a diameter of ca. 200 nm using a wrap-bake-peel method (Fig. 8a) [223]. It was observed that the TiO_2 wall exhibited a porous structure with a thickness of 25 nm. Due to the excellent porous and hollow structures, TOH exhibited a much larger BET surface area (228.6 m^2 g^{-1}) compared to that of TiO_2 nanoparticles (TON, 88.1 m^2 g^{-1}), resulting in a significant improvement of CO_2 adsorption capacity compared to TON (Fig. 8b). Correspondingly, the TOH exhibited much higher CO_2 reduction activity than TON. We used the activated carbon (AC) to modify TiO_2 and increase CO_2

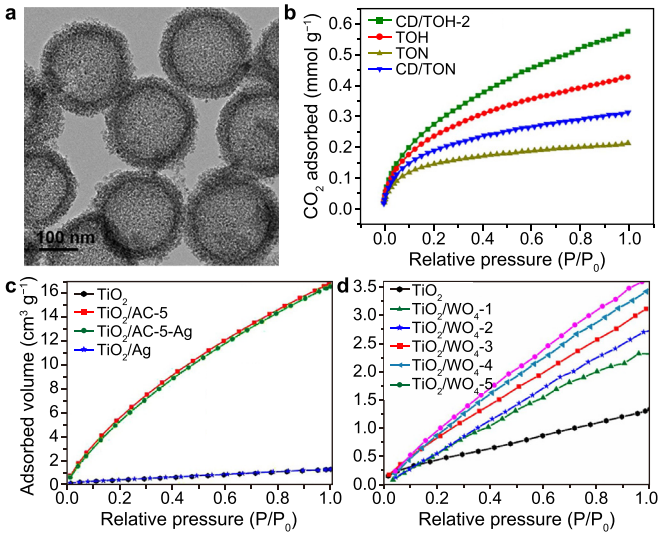

Fig. 8. **a**, TEM image of TOH. **b**, CO_2 adsorption isotherms on TOH and TON. **c**, CO_2 adsorption isotherms on TiO_2 and TiO_2/AC. **d**, CO_2 adsorption isotherms on TiO_2 and TiO_2/WO_4-X. Adapted with permission from Refs. [223–225]. Copyright 2021, 2018, 2019, Elsevier B.V.

adsorption capacity (Fig. 8c) [224]. The resulting TiO_2/AC exhibited six times higher activity than pure TiO_2 towards photocatalytic CO_2 reduction. Moreover, we designed a Lewis base $[WO_4]^{2-}$ to immobilize the TiO_2 surface [225]. Although the specific surface area (BET) of TiO_2 and TiO_2/WO_4-3 were similar, it was found that the CO_2 adsorption capacity of TiO_2 was significantly increased after the introduction of $[WO_4]^{2-}$ (Fig. 8d). It is well known that CO_2 is a weak Lewis acid, so Lewis base could favor the CO_2 adsorption. This should be the main role of $[WO_4]^{2-}$. Subsequently, the TiO_2/WO_4-3 exhibited excellent photocatalytic CO_2 to CO activity, much better than Ag/TiO_2 and Au/TiO_2. The enhancement of separation efficiency of photo-generated carriers due to the introduction of $[WO_4]^{2-}$ is another important factor.

3.3.4. Building surface frustrated lewis acid-base pair sites

Recently, constructing the frustrated Lewis pairs (FLPs) on the surface of photocatalysts has been proven to be a promising method to activate CO_2 molecules [226,227]. Typically, in a photocatalyst, the Lewis base could offer a lone electron pair, thereby coordinating the Lewis acid with an unoccupied orbital to generate a steady adduct. However, when there is a large steric hindrance, the coordination bonds between them cannot be generated, thereby forming an active region, that is, FLPs, rather than an acid-base adduct (Fig. 9) [71,228]. After the formation of FLPs, the Lewis acid with the unoccupied orbital could accept the lone pair electrons derived from the oxygen atom of CO_2. Non-bonding orbitals of Lewis base can donate electrons to the carbon atom of CO_2, thereby forming a s synergistic activation and dissociation effect for CO_2 molecules [229]. Therefore, the existence of FLPs could significantly improve the CO_2 photoreduction of photocatalysts.

Since 2016, when Ozin's group applied the FLPs theory to improve the CO_2 photoreduction of $In_2O_{3-x}(OH)_y$, FLPs quickly attracted the wide interest of CO_2 researchers [230]. Meanwhile, this strategy has been applied to modify TiO_2 to improve CO_2 photoreduction. Jia et al. [71] prepared hollow TiO_{2-x} boxes with FLPs active sites, in which the oxygen vacancies are considered as Lewis acid, and Lewis base is its proximal surface hydroxyl radicals. Because of the large steric hindrance between the vacancies and surface hydroxyl radicals, the FLPs have been formed [71]. The CO_2-

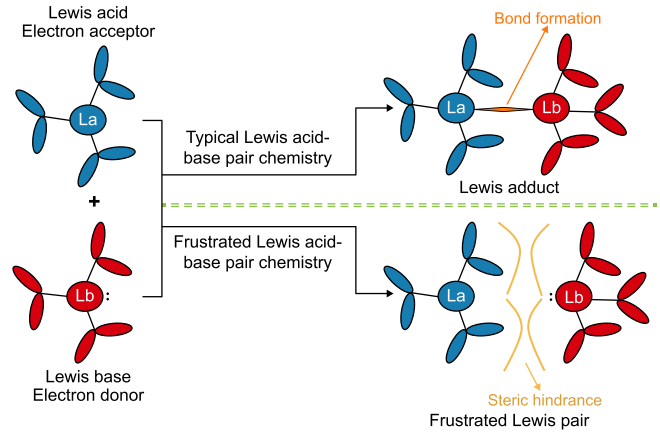

Fig. 9. Schematic diagram of the "typical Lewis acid-base chemistry" and "Frustrated Lewis pairs chemistry".

temperature programmed desorption (TPD) tests (Fig. 10a) confirmed that FLPs could improve the CO_2 adsorption capacity compared to pure TiO_2-A (hollow TiO_2 without FLP sites). Fig. 10b shows the Lewis acid (oxygen vacancies or Ti^{3+}) would link the oxygen atom of CO_2; meanwhile, the Lewis base (proximal surface hydroxyls) would bond to the carbon atom of CO_2, realizing the activation of the CO_2 molecule and reducing CO_2 adsorption energy of on the TiO_{2-x}. Therefore, the TiO_{2-x} sample exhibited a 19.1 times higher yield of CO than pure TiO_2-A (Fig. 10c and d).

4. *In situ* characterization and theoretical calculations

For photocatalytic CO_2 reduction, although a great deal of research studies have been made to upgrade the catalytic performance of the catalysts, it is still a challenge to design catalysts with desired activity and products because of the lack of understanding of the internal reaction progress and mechanism of CO reduction. To discover the mystery of CO_2 reduction, *in situ* characterization techniques were developed to monitor the transient kinetic process during the reaction [231]. Based on the results of various *in situ* characterizations, the building of theoretical calculation models can be more accurate, and the photocatalytic reaction mechanism will be clarified more clearly.

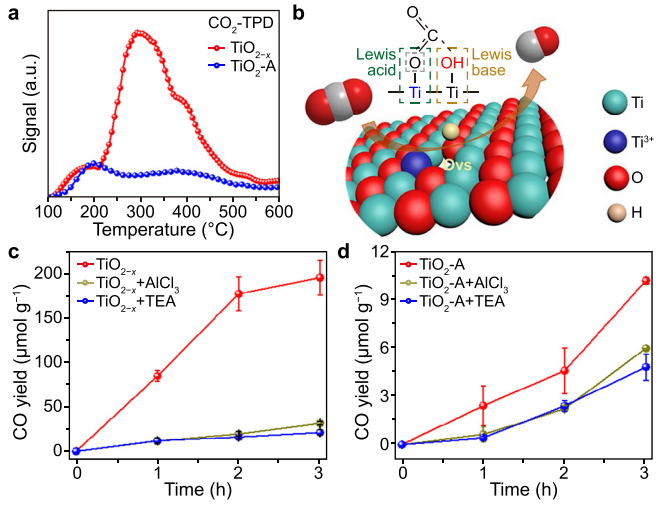

Fig. 10. **a**, CO_2-TPD of TiO_{2-x} and TiO_2-A. **b**, Schematic illustration of CO_2 reduction via TiO_{2-x}. **c**–**d**, Photocatalytic CO_2 reduction to CO activities via TiO_{2-x} **(c)** and TiO_2-A **(d)** samples. Adapted with permission from Ref. [71]. Copyright 2022, Elsevier B.V.

Recently, Dong's team reported the synergy effect of metal alloy nanoparticles (NPs) and single atoms (SAs), which can work together to maximize the catalytic performance. In this report, Cu SAs were successfully maintained on the surface of Au-Cu alloy NPs through a photo-deposition operation using TiO_2 photocatalyst [232]. Utilizing the advanced properties of Cu SAs and Au-Cu alloy NPs cocatalyst, the optimized photocatalyst showed photocatalytic CH_4 and C_2H_4 evolution activity using CO_2 and H_2O as reactants. The electron transfer progress during the photocatalytic reduction was studied by *in situ* irradiated XPS [232], and it found that the binding energy of Au 4f occurs a negative shift of about 0.3 eV, while the Ti 2p shift to the positive direction by 0.2 eV, meaning the transfer of electrons from TiO_2 to Au—Cu alloy under light irradiation. The *in situ* irradiated XPS (X-ray Photoelectron Spectroscopy) results can indicate that the metal cocatalyst is the final reactive site for the reaction. Besides, *in situ*, FT-IR spectra were further used to identify the transient reaction intermediated in the reaction progress. The *in situ* FT-IR spectra of $Cu_{0.8}Au_{0.2}/TiO_2$, Au/TiO_2, Cu/TiO_2, and TiO_2 were compared (Fig. S16). It was found that only in the *in situ* FT-IR spectra of $Cu_{0.8}Au_{0.2}/TiO_2$, C_2H_4* (at around 1440 and 1690 cm^{-1}) were observed, indicating the generation ability of C_2H_4 by $Cu_{0.8}Au_{0.2}/TiO_2$ photocatalyst.

Based on experimental conclusions, the DFT calculation was carried out to give the possible reaction routes in the photocatalytic CO_2 reaction progress (Fig. S17). Combing the results of experimental and DFT calculation, it was concluded that the C-C coupling progress between CH_2* and CH_2* rather than CO* and CO* coupling is the key to producing C_2H_4 for Cu SAs and Au-Cu alloy modified TiO_2 catalyst. The synergistic effect of Cu SAs and Au-Cu alloy decreases the activation barrier required for the CH_4 and C_2H_4 generation, thus largely promoting the evolution rate of CH_4 and C_2H_4 in the photocatalytic reduction of CO_2. In another work by Zhu and coauthors, the photocatalytic CO_2 reduction properties of Pd-porphyrin-based polymers coated hollow TiO_2 (Pd-HPP-TiO_2) were investigated [233]. By assembling Pd (II) sites into CO_2-adsorptive polymers and hollow TiO_2, CO_2 reduction progress using H_2O molecules as electron donors was achieved even in the aerobic environment. In this work, *in situ* FT-IR characterization was also used to elucidate the gas adsorption mechanism during the reaction. The CO_2 molecules are activated at Pd (II) sites and then reduced to the proton and photo-electron to form an *COOH intermediate. The reduction of *COOH into *CO can be finished by further reaction with the electron and proton. The generation of CO is achieved through the direct *CO desorption process. Meanwhile, part of the adsorbed *CO on Pd can be further reduced by the •H radicals in Pd-H species to generate CH_4 product.

Several kinds of *in situ* characterization techniques have been used to characterize the reaction mechanism, such as *in situ* ESR measurements, *in situ* Mass Spectrometry (MS), and *in situ* Raman. Recently, Sun's team gave a demonstration of using *in situ* electron paramagnetic resonance (EPR), affirming the real active site of Zr-MOF catalysts in photocatalytic CO_2, and it was proposed that both the organic ligands and the inorganic building unit could work as the reactive sites to boost the photocatalytic CO_2 reduction [234]. Regrettably, the application of other advanced *in situ* characterization techniques to study the photocatalytic CO_2 reduction mechanism of TiO_2-based catalysts remains limited. This limitation largely stems from the low activity of TiO_2 and the shortcomings of *in situ* characterization techniques. However, it is difficult for TiO_2 to exhibit satisfactory activity in practical photocatalytic CO_2 reduction applications due to the drawback of its wide band gap. They exhibited much better stability of TiO_2 than other nitrides, sulfides, and pure organic photocatalysts, making them a suitable model catalyst to explore the intrinsic mechanism of photocatalytic CO_2 under different conditions.

5. The O_2 evolution issue in photocatalytic CO_2 reduction

Based on the photocatalytic mechanism, an ideal photocatalytic CO_2 reduction progress should contain CO_2 reduction and H_2O oxidation. However, limited by the low efficiency, the use of hole scavenges, the low sensitivity of reaction equipment, and the impurity of the reaction CO_2 gas, the photocatalytic CO_2 reduction reaction along with O_2 evolution is rarely reported in TiO_2-based catalysts. A practical photocatalytic CO_2 reduction technique should prohibit using non-renewable hole scavengers unless more valuable oxidation products can be produced in this process. As an important component of artificial photosynthesis, the O_2 evolution reaction is one committed step to produce green energy using H_2O and CO_2 as reactants. Recently, single atoms modification presented a significant advantage in driving CO_2 reduction, water splitting, O_2 reduction, etc. In photocatalytic CO_2 reduction reaction, the surface constructed single atom sites can activate CO_2, adjusting the selectivity and accelerating the charges' separation. Jing and his coauthors reported a single Ni atom immobilized Ti-MOF and $BiVO_4$ (Ni@6MOF/BVO), which presented a nearly 100% CO selectivity and a greatly enhanced CO_2 reduction efficiency [235]. The presence of Ni single was confirmed with X-ray absorption near edge structure (XANES). In Ni@6MOF/BVO material, the Ni-Ni interaction in Ni metal was not found, confirming that the dispersion of Ni species is the single-atom state (Figs. S18a—c). The photocatalytic CO_2 reduction activity with H_2O as an electron donor was presented as shown in Figs. S18d and e. It is worth noting that the O_2 evolution was observed in the reaction, and the provided electrons by oxidizing H_2O are very close to the required electrons in CO_2 reduction, indicating the overall water splitting and CO_2 reduction progress. The achievement of overall water splitting is attributed to the S-scheme, which was proved by *in situ* XPS (Fig. S18 f—h). Another work from Jing presented a Zinc Phthalocyanine/$BiVO_4$ system with a Z-scheme electron-holes separation route, which obtained the purpose of O_2 evolution in photocatalytic CO_2 reduction, demonstrating the importance of the separation of oxidation and reduction sites [236].

6. Future perspectives and summary

In the past forty years, Over the past four decades, substantial research efforts have focused on enhancing the photocatalytic CO_2 efficiency of TiO_2 to meet emerging practical requirements. In this review, we have summarized current popular modification strategies toward TiO_2 from the viewpoints of crystal engineering, interface design, and reactive site construction. These methodologies delve into the optical properties, carrier migration behaviors, and active site design principles of TiO_2-based photocatalysts, aiming to adjust the activities and selectivity of CO_2 reduction products. Although the current activities of CO_2 photoreduction over TiO_2-based materials have been significantly enhanced compared to pure TiO_2, the efficiency remains suboptimal, indicating a significant gap for practical applications. Therefore, intensive investigations are still necessary to improve and optimize existing methods or develop new strategies to modify TiO_2. Such advancements are essential to realize its full potential for efficient, cost-effective, and sustainable deployment in practical applications.

(1) The preparation methods of TiO_2 are crucial, as they significantly influence its activity. In preparing TiO_2, it is necessary to avoid organic carbon pollution. Otherwise, carbon deposition will lead to the inactivation of TiO_2 during the photocatalytic CO_2 reduction. Furthermore, using environment-

friendly ("green") preparation methods is highly desirable under current environmental pressures.

(2) For many modification strategies, such as heterojunction construction, simply combining two materials improves the activity of TiO_2. However, existing research scarcely addresses the optimization of their interfacial connections. An excellent interface between the TiO_2 and another composite material can establish a low or negligible energy barrier between them, thus facilitating accelerated charge carrier transfer. Moreover, the intimate interface could effectively avoid separating two materials, maintaining the stability of the composite materials. Therefore, an excellent interface design is worthy of in-depth consideration in future research.

(3) In previous work, most researchers have studied the enhancement of TiO_2 activity from the views of physics direction, such as change of band gap, separation of charge carriers, crystal plane control, etc. However, there are limited studies on the chemical interactions, for instance, how the CO_2 molecule adsorbs to the surface of TiO_2-based composite photocatalysts. The recent introduction and developments of FLP theory provide good opportunities to model the photocatalytic activity considering chemical interactions and reactions. Therefore, combining the FLP method with other conventional methods (i.e., cocatalysts, crystal plane control) is an outstanding strategy.

(4) The photoreduction of CO_2 on TiO_2 involves two critical steps: reducing CO_2 by photo-generated electrons and oxidizing H_2O molecules through photo-generated holes. While most studies have focused extensively on the CO_2 reduction aspect, the oxidation of H_2O has received relatively less attention. Both reactions occur simultaneously, and the latter is also an important rate-determining step. Therefore, a thorough investigation of this oxidation process is essential for enhancing the photocatalytic CO_2 reduction activity of TiO_2.

(5) The excellent CB position enables TiO_2 to possess outstanding reductive ability toward CO_2, yet this also leads to the production of multiple potential products, posing a challenge in terms of low selectivity. Therefore, tuning the selectivity toward the target products is crucial. This optimization often involves lowering the reduction potentials of photo-generated electrons from the CB of modified TiO_2 materials at the expense of decreasing the reducing capability. Furthermore, exploring efficient ways to maintain the reductive ability of electrons from CB of TiO_2 and changing the CO_2 reaction path may be viable strategies to enhance selectivity tuning.

(6) The mechanisms underlying the photocatalytic reduction of CO_2 using TiO_2, as explored in many prior studies, have not been thoroughly investigated, primarily due to constraints imposed by experimental equipment. Photocatalytic CO_2 reduction using TiO_2-based catalysts is a complex multi-step reaction and presents significant challenges to fully elucidate the mechanism of the process. Recent advancements in various *in situ* spectroscopic techniques, such as *in situ* diffuse reflectance infrared Fourier transform spectroscopy, *in situ* attenuated total reflectance infrared spectroscopy, and other methods, provide opportunities to further explore the detailed reaction mechanism of photocatalytic CO_2 reduction. Combining these advanced analytical techniques and current theoretical DFT calculations can provide further insights into the mechanism of adsorption, desorption, formation of transient intermediate species, and energetics of the specific individual reaction steps in the process.

(7) The light adsorption properties of TiO_2-based catalysts are an important factor for the photocatalytic CO_2 reduction activity. To extend TiO_2 light absorption capacity, element doping and heterojunction construction strategies have shown obvious effectiveness. In general, these strategies enable the extension of the light absorption range of TiO_2 to extend to the visible region, but progress in the absorption of near-infrared light has been limited. Developing effective methods to further extend TiO_2's light absorption to near-infrared light for photocatalytic CO_2 reduction is an open field of research under the condition of maintaining sufficient carbon dioxide reduction capacity.

(8) Although the CO_2 photoreduction on the TiO_2 has been studied for several decades, the generated rates of products rarely reach the mmol g^{-1} h^{-1} range, mainly limited in the μmol g^{-1} h^{-1} range. This is far from the rate needed for actual industrial production. Considering a single modification strategy, it may enhance only one or a few specific capabilities of TiO_2 rather than all abilities. Thus, integrating multiple, effective modification strategies warrants further exploration to enhance the reaction efficiency. In this context, the potential benefits of incorporating photothermal synergy should also be thoroughly investigated.

Overall, CO_2 photoreduction on the TiO_2 still faces great challenges and is far behind the practical requirements. However, based on the increasingly serious problem of the CO_2 greenhouse effect, research into TiO_2-based CO_2 photoreduction holds considerable importance. It is imperative to persistently strive for its rapid advancement. A critical step in this endeavor is the comprehensive elucidation of the photocatalytic CO_2 reduction mechanism on TiO_2. A thorough understanding of this mechanism will enable the identification of the rate-limiting step in the reaction, thereby facilitating the rational design of highly efficient and targeted photocatalysts. This review aims to serve as a valuable resource on the mechanistic aspects and modification strategies of TiO_2 for photocatalytic CO_2 reduction and to inspire further research directed at mitigating greenhouse gas emissions.

CRediT authorship contribution statement

Zhimin Yuan: Conceptualization, Writing - Original Draft. **Xianglin Zhu:** Writing - Original Draft. **Xianqiang Gao:** Writing - Review & Editing. **Changhua An:** Writing - Review & Editing. **Zheng Wang:** Writing - Review & Editing. **Cheng Zuo:** Writing - Review & Editing. **Dionysios D. Dionysiou:** Writing - Review & Editing. **Hong He:** Conceptualization, Supervision, Writing - Review & Editing, Funding Acquisition. **Zaiyong Jiang:** Conceptualization, Supervision, Writing - Review & Editing, Funding Acquisition.

Declaration of competing interest

The authors declare that they have no known competing financial interests or personal relationships that could have appeared to influence the work reported in this paper.

Acknowledgements

This work was financially supported by the National Natural Science Foundation of China (22005123, 22188102), the Natural Science Foundation of Shandong Province, China (ZR2023MB049), China Postdoctoral Science Foundation (2020M670483), the Key Project of Natural Science Foundation of Tianjin City (Contract No. 22JCZDJC00510).

Appendix A. Supplementary data

Supplementary data to this article can be found online at https://doi.org/10.1016/j.ese.2023.100368.

References

[1] P.F. Zhang, K.S. Feng, L. Yan, Y.Q. Guo, B. Gao, J.S. Li, Overlooked CO_2 emissions induced by air pollution control devices in coal-fired power plants, Environ. Sci. Ecotechnol. 17 (2024) 100295.

[2] X.T. Zhang, T. Arbour, D.J. Zhang, S.Q. Wei, K. Rabaey, Microbial electrosynthesis of acetate from CO_2 under hypersaline conditions, Environ. Sci. Ecotechnol. 13 (2023) 100211.

[3] S.H. Wang, K. Feng, D.K. Zhang, D.R. Yang, M.Q. Xiao, C.C. Zhang, L. He, B.H. Yan, G.A. Ozin, W. Sun, Stable Cu catalysts supported by two-dimensional SiO_2 with strong metal–support interaction, Adv. Sci. 9 (2022) 2104972.

[4] G.A. Ozin, Accelerated optochemical engineering solutions to CO_2 photocatalysis for a sustainable future, Matter 5 (2022) 2594–2614.

[5] P.G. Obrien, K.K. Ghuman, A.A. Jelle, A. Sandhel, T.E. Wood, J.Y.Y. Loh, J. Jia, D. Perovic, C.V. Singh, N.P. Kherani, C.A. Mims, G.A. Ozin, Enhanced photothermal reduction of gaseous CO_2 over silicon photonic crystal supported ruthenium at ambient temperature, Energy Environ. Sci. 11 (2018) 3443–3451.

[6] G. Chen, R. Gao, Y. Zhao, Z. Li, G.I.N. Waterhouse, R. Shi, J. Zhao, M. Zhang, L. Shang, G. Sheng, X. Zhang, X. Wen, L.Z. Wu, C.H. Tung, T. Zhang, Alumina-supported CoFe alloy catalysts derived from layered-double-hydroxide nanosheets for efficient photothermal CO_2 hydrogenation to hydrocarbons, Adv. Mater. 30 (2018) 1704663.

[7] T.T. Zhao, Z.Y. Yang, Y.X. Tang, J.R. Liu, F.L. Wang, Advances and perspectives of photopromoted CO_2 hydrogenation for methane production: catalyst development and mechanism investigations, Energy Fuels 36 (2022) 6711–6735.

[8] J. Albero, Y. Peng, H. García, Photocatalytic CO_2 reduction to C2+ products, ACS Catal. 10 (2020) 5734–5749.

[9] J.L. Guo, Y. Liang, R. Song, J.Y.Y. Loh, N.P. Kherani, W. Wang, C. Kubel, Y. Dai, L. Wang, G.A. Ozin, Construction of new active sites: Cu substitution enabled surface frustrated lewis pairs over calcium hydroxyapatite for CO_2 hydrogenation, Adv. Sci. 8 (2021) 2101382.

[10] X.Y. Xiong, C.L. Mao, Z.J. Yang, Q.H. Zhang, G.I.N. Waterhouse, L. Gu, T.R. Zhang, Photocatalytic CO_2 reduction to CO over Ni single atoms supported on defect-rich zirconia, Adv. Energy Mater. 10 (2020) 2002928.

[11] R.G. Li, W.H. Cheng, M.H. Richter, J.S. Duchene, W.M. Tian, C. Li, H.A. Atwater, Unassisted highly selective gas-phase CO_2 reduction with a plasmonic Au/p-GaN photocatalyst using H_2O as an electron donor, ACS Energy Lett. 6 (2021) 1849–1856.

[12] J. Barrio, D. Mateo, J. Albero, H. Garcia, M. Shalom, A heterogeneous carbon nitride–nickel photocatalyst for efficient low-temperature CO_2 methanation, Adv. Energy Mater. 9 (2019) 1902738.

[13] Y. Wang, X.T. Shang, J.N. Shen, Z.Z. Zhang, D.B. Wang, J.J. Lin, J.C.S. Wu, X.Z. Fu, X.X. Wang, C. Li, Direct and indirect Z-scheme heterostructure-coupled photosystem enabling cooperation of CO_2 reduction and H_2O oxidation, Nat. Commun. 11 (2020) 3043.

[14] Z.H. Li, J.J. Liu, R. Shi, G.I.N. Waterhouse, X.D. Wen, T.R. Zhang, Fe-based catalysts for the direct photohydrogenation of CO_2 to value-added hydrocarbons, Adv. Energy Mater. 11 (2021) 2002783.

[15] X.P. Tao, Y. Wang, J.S. Qu, Y. Zhao, R.G. Li, C. Li, Achieving selective photocatalytic CO_2 reduction to CO on bismuth tantalum oxyhalogen nanoplates, J. Mater. Chem. A 9 (2021) 19631–19636.

[16] X.X. Chang, T. Wang, J.L. Gong, CO_2 photo-reduction: insights into CO_2 activation and reaction on surfaces of photocatalysts, Energy Environ. Sci. 9 (2016) 2177–2196.

[17] H.N. Huang, R. Shi, Z.H. Li, J.Q. Zhao, C.L. Su, T.R. Zhang, Triphase photocatalytic CO_2 reduction over silver-decorated titanium oxide at a gas-water boundary, Angew. Chem., Int. Ed. 134 (2022) e202200802.

[18] K. Torbensen, D. Joulie, S.X. Ren, M. Wang, D. Salvatore, C.P. Berlinguette, M. Robert, Molecular catalysts boost the rate of electrolytic CO_2 reduction, ACS Energy Lett. 5 (2020) 1512–1518.

[19] Y.F. Bao, S.W. Du, K.G. Shibata, X.Y. Guo, Y. Kamakura, Z.C. Feng, Y.Q. Huang, O. Ishitani, K. Maeda, F.X. Zhang, Layered β-ZrNBr nitro-halide as multifunctional photocatalyst for water splitting and CO_2 reduction, Angew. Chem., Int. Ed. 62 (2023) e202214273.

[20] M. Wang, K. Torbensen, D. Salvatore, S. Ren, D. Joulie, F. Dumoulin, D. Mendoza, B. Lassalle-Kaiser, U. Isci, CO_2 electrochemical catalytic reduction with a highly active cobalt phthalocyanine, Nat. Commun. 10 (2019) 3602.

[21] Y. Wang, R.Z. Liu, M. Shi, P.W. Zhou, K.L. Han, C. Li, R.G. Li, Photo-induced carbon dioxide reduction on hexagonal tungsten oxide via an oxygen vacancies-involved process, Chin. Chem. Lett. 34 (2023) 107200.

[22] M. Xing, Y. Zhou, C. Dong, L. Cai, L. Zeng, B. Shen, L. Pan, C. Dong, Y. Chai, J. Zhang, Y. Yin, Modulation of the reduction potential of TiO_{2-x} by fluorination for efficient and selective CH_4 generation from CO_2 photoreduction, Nano Lett. 18 (2018) 3384–3390.

[23] Y.X. Tang, T.T. Zhao, H.C. Han, Z.Y. Yang, J.R. Liu, X.D. Wen, F.L. Wang, Ir-CoO active centers supported on porous Al_2O_3 nanosheets as efficient and durable photo-thermal catalysts for CO_2 conversion, Adv. Sci. 10 (2023) 2300122.

[24] Z. Yan, J.L. Hitt, Z. Zeng, M.A. Hickner, T.E. Mallouk, Improving the efficiency of CO_2 electrolysis by using a bipolar membrane with a weak-acid cation exchange layer, Nat. Chem. 13 (2021) 33–40.

[25] X.L. Zhu, H.B. Zong, C.J.V. Perez, H.H. Miao, W. Sun, Z.M. Yuan, S.H. Wang, G.X. Zeng, H. Xu, Z.Y. Jiang, G.A. Ozin, Supercharged CO_2 photothermal catalytic methanation: high conversion, rate, and selectivity, Angew. Chem., Int. Ed. 62 (2023) e202218694.

[26] S. Remiro-Buenamañana, H. García, Photoassisted CO_2 conversion to fuels, ChemCatChem 11 (2018) 342–356.

[27] J.L. Hitt, Y.C. Li, S. Tao, Z. Yan, Y. Gao, S.J.L. Billinge, T.E. Mallouk, A high throughput optical method for studying compositional effects in electrocatalysts for CO_2 reduction, Nat. Commun. 12 (2021) 1114.

[28] H. Ou, S. Ning, P. Zhu, S. Chen, A. Han, Q. Kang, Z. Hu, J. Ye, D. Wang, Y. Li, Carbon nitride photocatalysts with integrated oxidation and reduction atomic active centers for improved CO_2 conversion, Angew. Chem. Int. Ed. 61 (2022) e202206579.

[29] H. Huang, H. Song, J. Kou, C. Lu, J. Ye, Atomic-level insights into surface engineering of semiconductors for photocatalytic CO_2 reduction, J. Energy Chem. 67 (2022) 309–341.

[30] L. Wang, R. Wang, T. Qiu, L. Yang, Q. Han, Q. Shen, X. Zhou, Y. Zhou, Z. Zou, Bismuth vacancy-induced efficient CO_2 photoreduction in BiOCl directly from natural air: a progressive step toward photosynthesis in nature, Nano Lett. 21 (2021) 10260–10266.

[31] Y.C. Li, D. Zhou, Z. Yan, R.H. Gonçalves, D.A. Salvatore, C.P. Berlinguette, T.E. Mallouk, Electrolysis of CO_2 to syngas in bipolar membrane-based electrochemical cells, ACS Energy Lett. 1 (2016) 1149–1153.

[32] X. Li, J. Yu, M. Jaroniec, X. Chen, Cocatalysts for selective photoreduction of CO_2 into solar fuels, Chem. Rev. 119 (2019) 3962–4179.

[33] H. Yu, R. Shi, Y. Zhao, G.I. Waterhouse, L.Z. Wu, C.H. Tung, T.R. Zhang, Smart utilization of carbon dots in semiconductor photocatalysis, Adv. Mater. 28 (2016) 9454–9477.

[34] R. Zeng, K. Lian, B. Su, L. Lu, J. Lin, D. Tang, S. Lin, X. Wang, Versatile synthesis of hollow metal sulfides via reverse cation exchange reactions for photocatalytic CO_2 reduction, Angew. Chem. Int. Ed. 60 (2021) 25055–25062.

[35] T. Inoue, A. Fujishima, S. Konishi, K. Honda, Photoelectrocatalytic reduction of carbon dioxide in aqueous suspensions of semiconductor powders, Nature 277 (1979) 637–638.

[36] J. Cheng, Y. Hou, K. Lian, H. Xiao, S. Lin, X. Wang, Metalized carbon nitrides for efficient catalytic functionalization of CO_2, ACS Catal. 12 (2022) 1797–1808.

[37] B. Yu, Y. Zhou, P. Li, W. Tu, P. Li, L. Tang, J. Ye, Z. Zou, Photocatalytic reduction of CO_2 over Ag/TiO_2 nanocomposites prepared with a simple and rapid silver mirror method, Nanoscale 8 (2016) 11870–11874.

[38] Y. Wang, X. Shang, J. Shen, Z. Zhang, D. Wang, J. Lin, J.C.S. Wu, X. Fu, X. Wang, C. Li, Direct and indirect Z-scheme heterostructure-coupled photosystem enabling cooperation of CO_2 reduction and H_2O oxidation, Nat. Commun. 11 (2020) 3043.

[39] R.R. Ikreedeegh, M. Tahir, A critical review in recent developments of metal-organic-frameworks (MOFs) with band engineering alteration for photocatalytic CO_2 reduction to solar fuels, J. CO_2 Util. 43 (2021) 101381.

[40] Z.Y. Jiang, X.Z. Liang, H.L. Zheng, Y.Y. Liu, Z.Y. Wang, P. Wang, X.Y. Zhang, X.Y. Qin, Y. Dai, M.H. Whangbo, B.B. Huang, Photocatalytic reduction of CO_2 to methanol by three-dimensional hollow structures of Bi_2WO_6 quantum dots, Appl. Catal. B Environ. 219 (2017) 209–215.

[41] M. Du, Y. Chen, W. Wang, X. Xu, Y. Li, Y. Zhang, Z. Li, Z. Zou, $A_2V_2O_7$ (A= Co, Ni, Cu and Zn) for CO_2 reduction under visible-light irradiation: effects of A site replacement, Appl. Catal. B Environ. 317 (2022) 121722.

[42] A. Wagner, C.D. Sahm, E. Reisner, Towards molecular understanding of local chemical environment effects in electro- and photocatalytic CO_2 reduction, Nat. Catal. 3 (2020) 775–786.

[43] Y. Dong, K.K. Ghuman, R. Popescu, P.N. Duchesne, W. Zhou, J.Y.Y. Loh, A.A. Jelle, J. Jia, D. Wang, X. Mu, C. Kubel, L. Wang, L. He, M. Ghoussoub, Q. Wang, T.E. Wood, L.M. Reyes, P. Zhang, N.P. Kherani, C.V. Singh, G.A. Ozin, Tailoring surface frustrated lewis pairs of $In_2O_{3-x}(OH)_y$ for gas-phase heterogeneous photocatalytic reduction of CO_2 by isomorphous substitution of In^{3+} with Bi^{3+}, Adv. Sci. 5 (2018) 1700732.

[44] M. Halmann, Photoelectrochemical reduction of aqueous carbon dioxide on p-type gallium phosphide in liquid junction solar cells, Nature 275 (1978) 115–116.

[45] L. Wang, W. Chen, D. Zhang, Y. Du, R. Amal, S. Qiao, J. Wu, Z. Yin, Surface strategies for catalytic CO_2 reduction: from two-dimensional materials to nanoclusters to single atoms, Chem. Soc. Rev. 48 (2019) 5310–5349.

[46] F. Xu, J. Zhang, B. Zhu, J. Yu, J. Xu, $CuInS_2$ sensitized TiO_2 hybrid nanofibers for improved photocatalytic CO_2 reduction, Appl. Catal. B Environ. 230 (2018) 194–202.

[47] Z. Jiang, W. Wan, H. Li, S. Yuan, H. Zhao, P.K. Wong, A hierarchical Z-scheme α-Fe_2O_3/g-C_3N_4 hybrid for enhanced photocatalytic CO_2 reduction, Adv. Mater. 30 (2018) 1706108.

[48] X.Y. Yue, L. Cheng, J.J. Fan, Q.J. Xiang, 2D/2D $BiVO_4$/$CsPbBr_3$ S-scheme heterojunction for photocatalytic CO_2 reduction: insights into structure regulation and Fermi level modulation, Appl. Catal. B Environ. 304 (2022) 120979.

[49] G. Zeng, J. Qiu, Z. Li, P. Pavaskar, S.B. Cronin, CO_2 reduction to methanol on

TiO_2-passivated GaP photocatalysts, ACS Catal. 4 (2014) 3512–3516.
[50] Y.P. Liu, D.Y. Shen, Q. Zhang, Y. Lin, F. Peng, Enhanced photocatalytic CO_2 reduction in H_2O vapor by atomically thin Bi_2WO_6 nanosheets with hydrophobic and nonpolar surface, Appl. Catal. B Environ. 283 (2021) 119630.
[51] Z.J. Chen, H. Guo, H.Y. Liu, C.G. Niu, D.W. Huang, Y.Y. Yang, C. Liang, L. Li, J.C. Li, Construction of dual S-scheme $Ag_2CO_3/Bi_4O_5I_2/g\text{-}C_3N_4$ heterostructure photocatalyst with enhanced visible-light photocatalytic degradation for tetracycline, Chem. Eng. J. 438 (2022) 135471.
[52] Y. Chen, D. Wang, X. Deng, Z. Li, Metal-organic frameworks (MOFs) for photocatalytic CO_2 reduction, Catal. Sci. Technol. 7 (2017) 4893–4904.
[53] S. Akrami, Y. Murakami, M. Watanabe, T. Ishihara, M. Arita, M. Fuji, K. Edalati, Defective high-entropy oxide photocatalyst with high activity for CO_2 conversion, Appl. Catal. B Environ. 303 (2022) 120896.
[54] P. Edalati, X.F. Shen, M. Watanabe, T. Ishihara, M. Arita, M. Fuji, K. Edalati, High-entropy oxynitride as a low-bandgap and stable photocatalyst for hydrogen production, J. Mater. Chem. A 9 (2021) 15076–15086.
[55] Y.J. Ma, Q. Tang, W.Y. Sun, Z.Y. Yao, W.H. Zhu, T. Li, J.Y. Wang, Assembling ultrafine TiO_2 nanoparticles on UiO-66 octahedrons to promote selective photocatalytic conversion of CO_2 to CH_4 at a low concentration, Appl. Catal. B Environ. 270 (2020) 118856.
[56] X.T. Hu, Z.J. Xie, Q. Tang, H. Wang, L.B. Zhang, J.Y. Wang, Enhanced CH_4 yields by interfacial heating-induced hot water steam during photocatalytic CO_2 reduction 298 (2021) 120635.
[57] S.L. Wang, M. Xu, T.Y. Peng, C.X. Zhang, T. Li, I. Hussain, J.Y. Wang, B. Tan, Porous hypercrosslinked polymer-TiO_2-graphene composite photocatalysts for visible-light-driven CO_2 conversion, Nat. Commun. 10 (2019) 676.
[58] Z.M. Yuan, Z.J. Jiang, Applications of BiOX in the photocatalytic reactions, Molecules 28 (11) (2023) 4400.
[59] Q. Li, Y. Xia, C. Yang, K. Lv, M. Lei, M. Li, Building a direct Z-scheme heterojunction photocatalyst by $ZnIn_2S_4$ nanosheets and TiO_2 hollowspheres for highly-efficient artificial photosynthesis, Chem. Eng. J. 349 (2018) 287–296.
[60] S. Wang, T.T. Zhao, Y. Tian, L.K. Yan, Z.M. Su, Mechanistic insight into photocatalytic CO_2 reduction by a Z-scheme $g\text{-}C_3N_4/TiO_2$ heterostructure, New J. Chem. 45 (2021) 11474–11480.
[61] Y. Zhou, Q. Zhang, X. Shi, Q. Song, C. Zhou, D. Jiang, Photocatalytic reduction of CO_2 into CH_4 over Ru-doped TiO_2: synergy of Ru and oxygen vacancies, J. Colloid Interface Sci. 608 (2022) 2809–2819.
[62] Y.H. Li, Z.T. Ren, M.L. Gu, Y.Y. Duan, W. Zhang, K.L. Lv, Synergistic effect of interstitial C doping and oxygen vacancies on the photoreactivity of TiO_2 nanofibers towards CO2 reduction, Appl. Catal. B Environ. 317 (2022) 121773.
[63] J.X. Low, S.Q. Qiu, D.F. Xu, C.J. Jiang, B. Cheng, Direct evidence and enhancement of surface plasmon resonance effect on Ag-loaded TiO_2 nanotube arrays for photocatalytic CO_2 reduction, Appl. Surf. Sci. 434 (2018) 423–432.
[64] G. Huang, Q. Shen, X. Ma, J. Zhong, J. Chen, J. Huang, L. Wang, H. She, Q. Wang, Preparation of an In_2S_3/TiO_2 heterostructure for enhanced activity in carbon dioxide photocatalytic reduction, ChemPhotoChem 5 (2021) 438–444.
[65] M.P. Jiang, K.K. Huang, J.H. Liu, D. Wang, Y. Wang, X. Wang, Z.D. Li, X.Y. Wang, Z.B. Geng, X.Y. Hou, S.H. Feng, Magnetic-field-regulated TiO_2 {100} facets: a strategy for CC coupling in CO_2 photocatalytic conversion, Chem 6 (2020) 2335–2346.
[66] X.G. Li, W.T. Bi, Z. Wang, W.G. Zhu, W.S. Chu, C.Z. Wu, Y. Xie, Surface-adsorbed ions on TiO_2 nanosheets for selective photocatalytic CO_2 reduction, Nano Res. 11 (2018) 3362–3370.
[67] F. Xu, K. Meng, B. Zhu, H. Liu, J. Xu, J. Yu, Graphdiyne: a new photocatalytic CO_2 reduction cocatalyst, Adv. Funct. Mater. 29 (2019) 1904256.
[68] J. Fu, S. Cao, J. Yu, J. Low, Y. Lei, Enhanced photocatalytic CO_2-reduction activity of electrospun mesoporous TiO_2 nanofibers by solvothermal treatment, Dalton Trans. 43 (2014) 9158–9165.
[69] Y. Ji, Y. Luo, New mechanism for photocatalytic reduction of CO_2 on the anatase TiO_2(101) surface: the essential role of oxygen vacancy, J. Am. Chem. Soc. 138 (2016) 15896–15902.
[70] H. Yu, S. Yan, P. Zhou, Z. Zou, CO_2 photoreduction on hydroxyl-group-rich mesoporous single crystal TiO_2, Appl. Surf. Sci. 427 (2018) 603–607.
[71] C. Jia, X. Kan, X. Zhang, G. Lin, W. Liu, Z. Wang, S. Zhu, D. Ju, J. Liu, Construction of frustrated Lewis pairs on TiO_{2-x} derived from perovskite for enhanced photocatalytic CO_2 reduction, Chem. Eng. J. 427 (2022) 131554.
[72] S. Kreft, D. Wei, H. Junge, M. Beller, Recent advances on TiO_2 based photocatalytic CO_2 reduction, Inside Energy 2 (2020) 100044.
[73] J.X. Low, B. Cheng, J.G. Yu, Surface modification and enhanced photocatalytic CO_2 reduction performance of TiO_2: a review, Appl. Surf. Sci. 392 (2017) 658–686.
[74] J. Wang, R.T. Guo, Z.X. Bi, X. Chen, X. Hu, W.G. Pan, A review on TiO_{2-x} based materials for photocatalytic CO_2 reduction, Nanoscale 14 (2022) 11512–11528.
[75] K.F. Li, X.Q. An, K.H. Park, M. Khraisheh, J.W. Tang, A critical review of CO_2 photoconversion: catalysts and reactors, Catal. Today 224 (2014) 3–12.
[76] S.W. Du, J.H. Lian, F.X. Zhang, Visible light-responsive N-doped TiO_2 photocatalysis: synthesis, characterizations, and applications, Trans. Tianjin Univ. 28 (2021) 33–52.
[77] X. Hu, R.T. Guo, X. Chen, Z.X. Bi, J. Wang, W.G. Pan, Bismuth-based Z-scheme structure for photocatalytic CO2 reduction: a review, J. Environ. Chem. Eng. 10 (2022) 108582.
[78] A. Sarkar, E. Gracia-Espino, T. Wagberg, A. Shchukarev, M. Mohl, A.R. Rautio, O. Pitkänen, T. Sharifi, K. Kordas, J.P. Mikkola, Photocatalytic reduction of CO_2 with H_2O over modified TiO_2 nanofibers: understanding the reduction pathway, Nano Res. 9 (2016) 1956–1968.
[79] J. Wu, H. Lu, X. Zhang, F. Raziq, Y. Qu, L. Jing, Enhanced charge separation of rutile TiO_2 nanorods by trapping holes and transferring electrons for efficient cocatalyst-free photocatalytic conversion of CO_2 to fuels, Chem. Commun. 52 (2016) 5027–5029.
[80] H. Lai, X. Zeng, T. Song, S. Yin, B. Long, A. Ali, G.J. Deng, Fast synthesis of porous iron doped CeO_2 with oxygen vacancy for effective CO_2 photoreduction, J. Colloid Interface Sci. 608 (2022) 1792–1801.
[81] S. Xie, Q. Zhang, G. Liu, Y. Wang, Photocatalytic and photoelectrocatalytic reduction of CO_2 using heterogeneous catalysts with controlled nanostructures, Chem. Commun. 52 (2016) 35–59.
[82] L.J. Liu, H.L. Zhao, J.M. Andino, Y. Li, Photocatalytic CO_2 reduction with H_2O on TiO_2 nanocrystals: comparison of anatase, rutile, and brookite polymorphs and exploration of surface chemistry, ACS Catal. 2 (2012) 1817–1828.
[83] H.J. Freund, M.W. Roberts, Surface chemistry of carbon dioxide, Surf. Sci. Rep. 25 (1996) 225–273.
[84] J.H. Xu, W.Z. Wang, S.M. Sun, L. Wang, Enhancing visible-light-induced photocatalytic activity by coupling with wide-band-gap semiconductor: a case study on Bi_2WO_6/TiO_2, Appl. Catal. B Environ. 111–112 (2012) 126–132.
[85] C.C. Mercado, F.J. Knorr, J.L. McHale, S.M. Usmani, A.S. Ichimura, L.V. Saraf, Location of hole and electron traps on nanocrystalline anatase TiO_2, J. Phys. Chem. C 116 (2012) 10796–10804.
[86] H.H. Mohamed, D.W. Bahnemann, The role of electron transfer in photocatalysis: fact and fictions, Appl. Catal. B Environ. 128 (2012) 91–104.
[87] R. Marschall, Semiconductor composites: strategies for enhancing charge carrier separation to improve photocatalytic activity, Adv. Funct. Mater. 24 (2014) 2421–2440.
[88] T. Hirakawa, P.V. Kamat, Charge separation and catalytic activity of Ag@TiO_2 core-shell composite clusters under UV-irradiation, J. Am. Chem. Soc. 127 (2005) 3928–3934.
[89] A. Cybula, M. Klein, A. Zaleska, Methane formation over TiO_2 based photocatalysts: reaction pathways, Appl. Catal. B Environ. 164 (2015) 433–442.
[90] S. Zhu, X.F. Chen, Z.C. Li, X.Y. Ye, Y. Liu, Y. Chen, L. Yang, M. Chen, D.Q. Zhang, G.S. Li, H.X. Li, Cooperation between inside and outside of TiO_2: lattice Cu^+ accelerates carrier migration to the surface of metal copper for photocatalytic CO_2 reduction, Appl. Catal. B Environ. 264 (2020) 118515.
[91] Y.H. Park, D. Kim, C.B. Hiragond, J. Lee, J.W. Jung, C.H. Cho, I. In, S.I. In, Phase-controlled 1T/2H-MoS_2 interaction with reduced TiO_2 for highly stable photocatalytic CO_2 reduction into CO, J. CO_2 Util. 67 (2023) 102324.
[92] Z.H. Zhang, J. Tan, L.S. Cheng, W.M. Yang, Carbon nano-layer coated TiO_2 nanoparticles for efficient photocatalytic CO_2 reduction into CH_4 and CO, Ceram. Int. 47 (2021) 34106–34114.
[93] X.L. Bao, M.H. Zhang, Z.Y. Wang, D.J. Dai, P. Wang, H.F. Cheng, Y.Y. Liu, Z.K. Zheng, Y. Dai, B.B. Huang, Molten-salt assisted synthesis of Cu clusters modified TiO_2 with oxygen vacancies for efficient photocatalytic reduction of CO_2 to CO, Chem. Eng. J. 445 (2022) 136718.
[94] M. Tahir, B. Tahir, Dynamic photocatalytic reduction of CO_2 to CO in a honeycomb monolith reactor loaded with Cu and N doped TiO_2 nanocatalysts, Appl. Surf. Sci. 377 (2016) 244–252.
[95] H.B. Yin, F. Dong, D.S. Wang, J.H. Li, Coupling Cu single atoms and phase junction for photocatalytic CO_2 reduction with 100% CO selectivity, ACS Catal. 12 (2022) 14096–14105.
[96] M.S. Choe, S. Choi, S.Y. Kim, C. Back, D. Lee, H.S. Lee, C.H. Kim, H.J. Son, S.O. Kang, A hybrid Ru(II)/TiO_2 catalyst for steadfast photocatalytic CO_2 to CO/formate conversion following a molecular catalytic route, Inorg. Chem. 60 (2021) 10235–10248.
[97] Y.F. Miao, R.T. Guo, J.W. Gu, Y.Z. Liu, G.L. Wu, C.P. Duan, W.G. Pan, Z-scheme $Bi/Bi_2O_2CO_3$/layered double-hydroxide nanosheet heterojunctions for photocatalytic CO_2 reduction under visible light, ACS Appl. Nano Mater. 4 (2021) 4902–4911.
[98] C.Y. Huang, R.T. Guo, W.G. Pan, J.Y. Tang, W.G. Zhou, H. Qin, X.Y. Liu, P.Y. Jia, Eu-doped TiO_2 nanoparticles with enhanced activity for CO_2 phpotcatalytic reduction, J. CO_2 Util. 26 (2018) 487–495.
[99] J.J. Walsh, C. Jiang, J. Tang, A.J. Cowan, Photochemical CO_2 reduction using structurally controlled $g\text{-}C_3N_4$, Phys. Chem. Chem. Phys. 18 (2016) 24825–24829.
[100] Y. Wang, E. Chen, J.W. Tang, Insight on reaction pathways of photocatalytic CO_2 conversion, ACS Catal. 12 (2022) 7300–7316.
[101] M.S. Akple, J.X. Low, Z.Y. Qin, S. Wageh, A.A. Al-Ghamdi, J.G. Yu, S.W. Liu, Nitrogen-doped TiO_2 microsheets with enhanced visible light photocatalytic activity for CO_2 reduction, Chin. J. Catal. 36 (2015) 2127–2134.
[102] L.M. Xue, F.H. Zhang, H.J. Fan, X.F. Bai, Preparation of C Doped TiO_2 photocatalysts and their photocatalytic reduction of carbon dioxide, Adv. Mater. Res. 183–185 (2011) 1842–1846.
[103] Q.Y. Zhang, Y. Li, E.A. Ackerman, M. Gajdardziska-Josifovska, H.L. Li, Visible light responsive iodine-doped TiO_2 for photocatalytic reduction of CO_2 to fuels, Appl. Catal. A-Gen. 400 (2011) 195–202.
[104] O.R. Andrade, V. Rodriguez, R. Camarillo, F. Martinez, C. Jimenez, J. Rincon, Photocatalytic reduction of CO_2 with N-doped TiO_2-based photocatalysts obtained in one-pot supercritical synthesis, Nanomaterials 12 (2022) 1793.

[105] K.D. Wang, J. Yu, L.J. Liu, L. Hou, F.Y. Jin, Hierarchical P-doped TiO_2 nanotubes array@Ti plate: towards advanced CO_2 photocatalytic reduction catalysts, Ceram. Int. 42 (2016) 16405–16411.
[106] N.R. Khalid, E. Ahmed, N.A. Niaz, G. Nabi, M. Ahmad, M.B. Tahir, M. Rafique, M. Rizwan, Y. Khan, Highly visible light responsive metal loaded N/TiO_2 nanoparticles for photocatalytic conversion of CO_2 into methane, Ceram. Int. 43 (2017) 6771–6777.
[107] S.A. Ansari, M.M. Khan, M.O. Ansari, M.H. Cho, Nitrogen-doped titanium dioxide (N-doped TiO_2) for visible light photocatalysis, New J. Chem. 40 (2016) 3000–3009.
[108] X.K. Li, Z.J. Zhuang, W. Li, H.Q. Pan, Photocatalytic reduction of CO_2 over noble metal-loaded and nitrogen-doped mesoporous TiO_2, APPL CATAL A-GEN 429–430 (2012) 31–38.
[109] X.Y. Wang, Z.G. Zhang, Z.F. Huang, P.M. Dong, X.X. Nie, Z. Jin, X.W. Zhang, Synergistic effect of N-Ho on photocatalytic CO_2 reduction for N/Ho co-doped TiO_2 nanorods, Mater. Res. Bull. 118 (2019) 110502.
[110] A. Bjelajac, D. Kopač, A. Fecant, E. Tavernier, R. Petrović, B. Likozar, D. Janaćković, Micro-kinetic modelling of photocatalytic CO_2 reduction over undoped and N-doped TiO_2, Catal. Sci. Technol. 10 (6) (2020) 1688–1698.
[111] N.U.M. Nor, N.A.S. Amin, Glucose precursor carbon-doped TiO_2 heterojunctions for enhanced efficiency in photocatalytic reduction of carbon dioxide to methanol, J. CO_2 Util. 33 (2019) 372–383.
[112] F. Feng, W.Y. Yang, S. Gao, C.X. Sun, Q. Li, Postillumination activity in a single-phase photocatalyst of Mo-doped TiO_2 nanotube array from its photocatalytic "memory", ACS Sustain. Chem. Eng. 6 (5) (2018) 6166–6174.
[113] Z. Xiong, Z.W. Xu, Y.Z. Li, L.C. Dong, J.Y. Wang, J.T. Zhao, X.X. Chen, Y.C. Zhao, H.B. Zhao, J.Y. Zhang, Incorporating highly dispersed and stable Cu^+ into TiO_2 lattice for enhanced photocatalytic CO_2 reduction with water, Appl. Surf. Sci. 507 (2020) 145095.
[114] C.Y. Huang, R.T. Guo, W.G. Pan, J.Y. Tang, W.G. Zhou, X.Y. Liu, H. Qin, P.Y. Jia, One-dimension TiO_2 nanostructures with enhanced activity for CO_2 photocatalytic reduction, Appl. Surf. Sci. 464 (2019) 534–543.
[115] M. Tahir, N.S. Amin, Indium-doped TiO_2 nanoparticles for photocatalytic CO_2 reduction with H_2O vapors to CH_4, Appl. Catal., B 162 (2015) 98–109.
[116] Z. Xiong, Z. Lei, S.M. Ma, X.X. Chen, B.G. Gong, Y.C. Zhao, J.Y. Zhang, C.G. Zheng, J.C.S. Wu, Photocatalytic CO_2 reduction over V and W codoped TiO_2 catalyst in an internal-illuminated honeycomb photoreactor under simulated sunlight irradiation, Appl. Catal., B 219 (2017) 412–424.
[117] R. Camarillo, D. Rizaldos, C. Jiménez, F. Martínez, J. Rincón, Enhancing the photocatalytic reduction of CO_2 with undoped and Cu-doped TiO_2 nanofibers synthesized in supercritical medium, J. Supercrit. Fluids 147 (2019) 70–80.
[118] X.H. Feng, F.P. Pan, P. Zhang, X. Wang, H.C. Zhou, Y.H. Huang, Y. Li, Metal-organic framework MIL-125 derived Mg^{2+}-doped mesoporous TiO_2 for photocatalytic CO_2 reduction, ChemPhotoChem 5 (1) (2020) 79–89.
[119] M. Xu, H. Wu, Y.W. Tang, G.B. Mao, G. Wang, L. Zhang, Q. Liu, One-step in-situ synthesis of porous Fe^{3+}-doped TiO_2 octahedra toward visible-light photocatalytic conversion of CO_2 into solar fuel, Microporous Mesoporous Mater. 309 (2020) 110539.
[120] S.J. Feng, J. Zhao, Y.J. Bai, X.X. Liang, T. Wang, C.Y. Wang, Facile synthesis of Mo-doped TiO_2 for selective photocatalytic CO_2 reduction to methane: promoted H_2O dissociation by Mo doping, J. CO_2 Util. 38 (2020) 1–9.
[121] Z.J. Chen, J.Y. Xiong, G. Cheng, Recent advances in brookite phase TiO_2-based photocatalysts toward CO_2 reduction, Fuel 357 (2024) 129806.
[122] X. Chen, L. Liu, P.Y. Yu, S.S. Mao, Increasing solar absorption for photocatalysis with black hydrogenated titanium dioxide nanocrystals, Science 331 (2011) 746–750.
[123] M. Niu, D. Cheng, D. Cao, Fluorite TiO_2(111) surface phase for enhanced visible-light solar energy conversion, J. Phys. Chem. C 118 (2014) 20107–20111.
[124] H. Razavi-Khosroshahi, K. Edalati, M. Hirayama, H. Emami, M. Arita, M. Yamanuchi, H. Hagiwara, S. Ida, T. Ishihara, E. Akiba, Z.J. Horita, M. Fuji, Visible-light-driven photocatalytic hydrogen generation on nanosized TiO_2-II stabilized by high-pressure torsion, ACS Catal. 6 (2016) 5103–5107.
[125] Q. Wang, M. Watanabe, K. Edalati, Visible-light photocurrent in nanostructured high-pressure TiO_2-II (columbite) phase, J. Phys. Chem. C 124 (2020) 13930–13935.
[126] S. Akrami, M. Watanabe, T.H. Ling, T. Ishihara, M. Arita, M. Fuji, K. Edalati, High-pressure TiO_2-II polymorph as an active photocatalyst for CO_2 to CO conversion, Appl. Catal. B Environ. 298 (2021) 120566.
[127] A. Ziarati, A. Badiei, R. Luque, M. Dadras, T. Burgi, Visible light CO_2 reduction to CH_4 using hierarchical yolk@shell $TiO_{2-x}H_x$ modified with plasmonic Au–Pd nanoparticles, ACS Sustain. Chem. Eng. 8 (9) (2020) 3689–3696.
[128] J.X. Low, L.Y. Zhang, B.C. Zhu, Z.Y. Liu, J.G. Yu, TiO_2 photonic crystals with localized surface photothermal effect and enhanced photocatalytic CO_2 reduction activity, ACS Sustain. Chem. Eng. 6 (11) (2018) 15653–15661.
[129] I. Hashemizadeh, V.B. Golovko, J. Choi, D.C.W. Tsang, A.C.K. Yip, Photocatalytic reduction of CO_2 to hydrocarbons using bio-templated porous TiO_2 architectures under UV and visible light, Chem. Eng. J. 347 (2018) 64–73.
[130] L.C. Dong, Z. Xiong, Y.M. Zhou, J.T. Zhao, Y.Z. Li, J.Y. Wang, X.X. Chen, Y.C. Zhao, J.Y. Zhang, Photocatalytic CO_2 reduction over postcalcinated atomically thin TiO_2 nanosheets: residual carbon removal and structure transformation, J. CO_2 Util. 41 (2020) 101262.
[131] K. Alkanad, A. Hezam, N. Al-Zaqri, M.A. Bajiri, G. Alnaggar, Q.A. Drmosh, H.A. Almukhlifi, L. Neratur Krishnappagowda, One-step hydrothermal synthesis of anatase TiO_2 nanotubes for efficient photocatalytic CO_2 reduction, ACS Omega 7 (43) (2022) 38686–38699.
[132] T.M. Di, J.F. Zhang, B. Cheng, J.G. Yu, J.S. Xu, Hierarchically nanostructured porous TiO_2(B) with superior photocatalytic CO_2 reduction activity, Sci. China Chem. 61 (3) (2018) 344–350.
[133] P. Reñones, A. Moya, F. Fresno, L. Collado, J.J. Vilatela, V.A. de la Peña O'Shea, Hierarchical TiO_2 nanofibres as photocatalyst for CO_2 reduction: influence of morphology and phase composition on catalytic activity, J. CO_2 Util. 15 (2016) 24–31.
[134] Q.D. Truong, H.T. Hoa, T.S. Le, Rutile TiO_2 nanocrystals with exposed {331} facets for enhanced photocatalytic CO_2 reduction activity, J. Colloid Interface Sci. 504 (2017) 223–229.
[135] K. Kočí, L. Obalová, L. Matějová, D. Plachá, Z. Lacný, J. Jirkovský, O. Šolcová, Effect of TiO_2 particle size on the photocatalytic reduction of CO_2, Appl. Catal., B 89 (3–4) (2009) 494–502.
[136] J. Yu, J. Low, W. Xiao, P. Zhou, M. Jaroniec, Enhanced photocatalytic CO_2 reduction activity of anatase TiO_2 by coexposed {001} and {101} facets, J. Am. Chem. Soc. 136 (25) (2014) 8839–8842.
[137] F. Fang, Y.X. Liu, X. Sun, C. Fu, Y. Prakash Bhoi, W. Xiong, W.X. Huang, TiO_2 facet-dependent reconstruction and photocatalysis of CuO_x/TiO_2 photocatalysts in CO_2 photoreduction, Appl. Surf. Sci. 564 (2021) 150407.
[138] A. Meng, L. Zhang, B. Cheng, J. Yu, TiO_2-MnO_x-Pt hybrid multiheterojunction film photocatalyst with enhanced photocatalytic CO_2 reduction activity, ACS Appl. Mater. Interfaces 11 (6) (2019) 5581–5589.
[139] C. Zhu, Y. Shen, F. Yang, P. Zhu, C.H. An, Engineering hydrogenated TiO_2 nanosheets by rational deposition of Ni clusters and Pt single atoms onto exposing facets for high-performance solar fuel production, Chem. Eng. J. 466 (2023) 143174.
[140] A. Banitalebi Dehkordi, A. Ziarati, J.B. Ghasemi, A. Badiei, Preparation of hierarchical g-C_3N_4@TiO_2 hollow spheres for enhanced visible-light induced catalytic CO_2 reduction, Sol. Energy 205 (2020) 465–473.
[141] H.Q. Wang, H.D. Li, Z.W. Chen, J.Z. Li, X. Li, P.W. Huo, Q. Wang, TiO_2 modified g-C_3N_4 with enhanced photocatalytic CO_2 reduction performance, Solid State Sci. 100 (2020) 106099.
[142] K. Li, B.S. Peng, J.P. Jin, L. Zan, T.Y. Peng, Carbon nitride nanodots decorated brookite TiO_2 quasi nanocubes for enhanced activity and selectivity of visible-light-driven CO_2 reduction, Appl. Catal., B 203 (2017) 910–916.
[143] A. Crake, K.C. Christoforidis, A. Kafizas, S. Zafeiratos, C. Petit, CO_2 capture and photocatalytic reduction using bifunctional TiO_2/MOF nanocomposites under UV–vis irradiation, Appl. Catal., B 210 (2017) 131–140.
[144] Y.X. Gao, Z.K. Tan, R. Yang, G.C. Huang, J.H. Bi, Integrating polyarylether-COFs with TiO_2 nanofibers for enhanced visible-light-driven CO_2 reduction in artificial photosynthesis, Appl. Surf. Sci. 605 (2022) 154605.
[145] H. Maimaiti, A. Awati, G. Yisilamu, D. Zhang, S. Wang, Synthesis and visible-light photocatalytic CO_2/H_2O reduction to methyl formate of TiO_2 nanoparticles coated by aminated cellulose, Appl. Surf. Sci. 466 (2019) 535–544.
[146] H.C. Yang, H.Y. Lin, Y.S. Chien, J.C.S. Wu, H.H. Wu, Mesoporous TiO_2/SBA-15, and Cu/TiO_2/SBA-15 composite photocatalysts for photoreduction of CO_2 to methanol, Catal. Lett. 131 (3–4) (2009) 381–387.
[147] C.Y. Zhao, L.J. Liu, Q.Y. Zhang, J. Wang, Y. Li, Photocatalytic conversion of CO_2 and H_2O to fuels by nanostructured Ce–TiO_2/SBA-15 composites, Catal. Sci. Technol. 2 (12) (2012) 2558.
[148] B. Srinivas, B. Shubhamangala, K. Lalitha, P.A. Reddy, V.D. Kumari, M. Subrahmanyam, B.R. De, Photocatalytic reduction of CO_2 over Cu-TiO_2/molecular sieve 5A composite, Photochem. Photobiol. 87 (5) (2011) 995–1001.
[149] Y.L. Yang, D.N. Zhang, J.J. Fan, Y.L. Liao, Q.J. Xiang, Construction of an ultrathin S-scheme heterojunction based on few-layer g-C_3N_4 and monolayer $Ti_3C_2T_x$ MXene for photocatalytic CO_2 reduction, Sol. RRL 5 (2) (2020) 2000351.
[150] Z.L. Dong, Z.J. Zhang, Y. Jiang, Y.Q. Chu, J.Y. Xu, Embedding $CsPbBr_3$ perovskite quantum dots into mesoporous TiO_2 beads as an S-scheme heterojunction for CO_2 photoreduction, Chem. Eng. J. 433 (2022) 133762.
[151] F. Iqbal, A. Mumtaz, S. Shahabuddin, M.I. Abd Mutalib, M.S. Shaharun, T.D. Nguyen, M.R. Khan, B. Abdullah, Photocatalytic reduction of CO_2 to methanol over $ZnFe_2O_4/TiO_2$ (p–n) heterojunctions under visible light irradiation, J. Chem. Technol. Biotechnol. 95 (8) (2020) 2208–2221.
[152] F. Xu, K. Meng, B. Cheng, S. Wang, J. Xu, J. Yu, Unique S-scheme heterojunctions in self-assembled $TiO_2/CsPbBr_3$ hybrids for CO_2 photoreduction, Nat. Commun. 11 (1) (2020) 4613.
[153] J. Low, J. Yu, M. Jaroniec, S. Wageh, A.A. Al-Ghamdi, Heterojunction photocatalysts, Adv. Mater. 29 (20) (2017) 1601694.
[154] E. Kim, K.H. Do, J. Wang, Y. Hong, A. Putta Rangappa, D. Amaranatha Reddy, D. Praveen Kumar, T.K. Kim, Construction of 1D TiO_2 nanotubes integrated ultrathin 2D $ZnIn_2S_4$ nanosheets heterostructure for highly efficient and selective photocatalytic CO_2 reduction, Appl. Surf. Sci. 587 (2022) 152895.
[155] G. Yang, P. Qiu, J.Y. Xiong, X.T. Zhu, G. Cheng, Facilely anchoring Cu_2O nanoparticles on mesoporous TiO_2 nanorods for enhanced photocatalytic CO_2 reduction through efficient charge transfer, Chin. Chem. Lett. 33 (8) (2022) 3709–3712.
[156] S.P. Cheng, L.W. Wei, H.P. Wang, Photocatalytic reduction of CO_2 to methanol by Cu_2O/TiO_2 heterojunctions, Sustainability 14 (1) (2021) 374.
[157] Y. Ke, Q. Liang, S. Zhao, Z.H. Zhang, X.Z. Li, Z.Y. Li, In situ self-assembled ZIF-67/MIL-125-derived Co_3O_4/TiO_2 p–n heterojunctions for enhanced photocatalytic CO_2 reduction, Inorg. Chem. 61 (5) (2022) 2652–2661.
[158] Y. Jiang, H.Y. Chen, J.Y. Li, J.F. Liao, H.H. Zhang, X.D. Wang, D.B. Kuang, Z-scheme 2D/2D heterojunction of $CsPbBr_3/Bi_2WO_6$ for improved

photocatalytic CO_2 reduction, Adv. Funct. Mater. 30 (50) (2020) 2004293.
[159] J. Wu, Y.J. Feng, D. Li, X.Y. Han, J. Liu, Efficient photocatalytic CO_2 reduction by P−O linked g-C_3N_4/TiO_2-nanotubes Z-scheme composites, Energy 178 (2019) 168−175.
[160] G. Marcì, E.I. García-López, L. Palmisano, Photocatalytic CO_2 reduction in gas−solid regime in the presence of H_2O by using GaP/TiO_2 composite as photocatalyst under simulated solar light, Catal. Commun. 53 (2014) 38−41.
[161] Z.U. Rehman, M. Bilal, J. Hou, F.K. Butt, J. Ahmad, S. Ali, A. Hussain, Photocatalytic CO_2 reduction using TiO_2-based photocatalysts and TiO_2 Z-scheme heterojunction composites: a review, Molecules 27 (7) (2022) 2069.
[162] X.N. Wang, Z.L. Jiang, H.W. Chen, K. Wang, X.T. Wang, Photocatalytic CO_2 reduction with water vapor to CO and CH_4 in a recirculation reactor by Ag-Cu_2O/TiO_2 Z-scheme heterostructures, J. Alloys Compd. 896 (2022) 163030.
[163] G.X. Song, F. Xin, J.S. Chen, X.H. Yin, Photocatalytic reduction of CO_2 in cyclohexanol on CdS−TiO_2 heterostructured photocatalyst, APPL CATAL A-GEN 473 (2014) 90−95.
[164] M. Tahir, Well-designed $ZnFe_2O_4$/Ag/TiO_2 nanorods heterojunction with Ag as electron mediator for photocatalytic CO_2 reduction to fuels under UV/visible light, J. CO_2 Util. 37 (2020) 134−146.
[165] G.H. Li, Y.Y. Sun, Q.M. Zhang, Z. Gao, W. Sun, X.X. Zhou, Ag quantum dots modified hierarchically porous and defective TiO_2 nanoparticles for improved photocatalytic CO_2 reduction, Chem. Eng. J. 410 (2021) 128397.
[166] A. Pougin, G. Dodekatos, M. Dilla, H. Tuysuz, J. Strunk, Au@TiO_2 core-shell composites for the photocatalytic reduction of CO_2, Chem. Eur J. 24 (47) (2018) 12416−12425.
[167] R. Wang, J. Shen, K.H. Sun, H. Tang, Q. Liu, Enhancement in photocatalytic activity of CO_2 reduction to CH_4 by 0D/2D Au/TiO_2 plasmon heterojunction, Appl. Surf. Sci. 493 (2019) 1142−1149.
[168] M. Tahir, B. Tahir, N.A.S. Amin, Gold-nanoparticle-modified TiO_2 nanowires for plasmon-enhanced photocatalytic CO_2 reduction with H_2 under visible light irradiation, Appl. Surf. Sci. 356 (2015) 1289−1299.
[169] R. Tang, H.Y. Sun, Z.Y. Zhang, L. Liu, F.N. Meng, X.M. Zhang, W.J. Yang, Z.T. Li, Z.F. Zhao, R.K. Zheng, J. Huang, Incorporating plasmonic Au-nanoparticles into three-dimensionally ordered macroporous perovskite frameworks for efficient photocatalytic CO_2 reduction, Chem. Eng. J. 429 (2022) 132137.
[170] E.Z. Liu, Y. Hu, H. Li, C.N. Tang, X.Y. Hu, J. Fan, Y.H. Chen, J.J. Bian, Photoconversion of CO_2 to methanol over plasmonic Ag/TiO_2 nano-wire films enhanced by overlapped visible-light-harvesting nanostructures, Ceram. Int. 41 (1) (2015) 1049−1057.
[171] F. Khatun, A. Abd Aziz, L.C. Sim, M.U. Monir, Plasmonic enhanced Au decorated TiO_2 nanotube arrays as a visible light active catalyst towards photocatalytic CO_2 conversion to CH_4, J. Environ. Chem. Eng. 7 (6) (2019) 103233.
[172] P. Reñones, L. Collado, A. Iglesias-Juez, F.E. Oropeza, F. Fresno, V.A. de la Peña O'Shea, Silver−gold bimetal-loaded TiO_2 photocatalysts for CO_2 reduction, Ind. Eng. Chem. Res. 59 (20) (2020) 9440−9450.
[173] Q.L. Wang, P.M. Dong, Z.F. Huang, X.W. Zhang, Synthesis of Ag or Pt nanoparticle-deposited TiO_2 nanorods for the highly efficient photoreduction of CO_2 to CH_4, Chem. Phys. Lett. 639 (2015) 11−16.
[174] M.Y. Wang, X.C. Pang, D.J. Zheng, Y.J. He, L. Sun, C.J. Lin, Z.Q. Lin, Nonepitaxial growth of uniform and precisely size-tunable core/shell nanoparticles and their enhanced plasmon-driven photocatalysis, J. Mater. Chem. A 4 (19) (2016) 7190−7199.
[175] J.T. Li, S.K. Cushing, F.K. Meng, T.R. Senty, A.D. Bristow, N.Q. Wu, Plasmon-induced resonance energy transfer for solar energy conversion, Nat. Photonics 9 (9) (2015) 601−607.
[176] Y.C. Yao, X.R. Dai, X.Y. Hu, S.Z. Huang, Z. Jin, Synthesis of Ag-decorated porous TiO_2 nanowires through a sunlight induced reduction method and its enhanced photocatalytic activity, Appl. Surf. Sci. 387 (2016) 469−476.
[177] K. Awazu, M. Fujimaki, C. Rockstuhl, J. Tominaga, H. Murakami, Y. Ohki, N. Yoshida, T. Watanabe, A plasmonic photocatalyst consisting of silver nanoparticles embedded in titanium dioxide, J. Am. Chem. Soc. 130 (5) (2008) 1676−1680.
[178] M. Tahir, B. Tahir, N.A.S. Amin, Z.Y. Zakaria, Photo-induced reduction of CO_2 to CO with hydrogen over plasmonic Ag-NPs/TiO_2 NWs core/shell heterojunction under UV and visible light, J. CO_2 Util. 18 (2017) 250−260.
[179] K. Zhang, Y.W. Dai, Z.H. Zhou, S. Ullah Jan, L.J. Guo, J.R. Gong, Polarization-induced saw-tooth-like potential distribution in zincblende-wurtzite superlattice for efficient charge separation, Nano Energy 41 (2017) 101−108.
[180] Y. Fan, X. Song, H. Ai, W. Li, M. Zhao, Highly efficient photocatalytic CO_2 reduction in two-dimensional ferroelectric $CuInP_2S_6$ bilayers, ACS Appl. Mater. Interfaces 13 (29) (2021) 34486−34494.
[181] W. Wang, B. Huang, X. Ma, Z. Wang, X. Qin, X. Zhang, Y. Dai, M.H. Whangbo, Efficient separation of photogenerated electron-hole pairs by the combination of a heterolayered structure and internal polar field in pyroelectric $BiOIO_3$ nanoplates, Chem. Eur J. 19 (44) (2013) 14777−14780.
[182] M.N. Chu, Y. Li, K. Cui, J.H. Jian, S.T. Lu, P. Gao, X.H. Wu, Enhanced photocatalytic reduction of carbon dioxide into carbon monoxide by electric field generation and defect engineering in TiO_2, Environ. Chem. Lett. 20 (2) (2022) 999−1007.
[183] L. Jin, E. Shaaban, S. Bamonte, D. Cintron, S. Shuster, L. Zhang, G. Li, J. He, Surface basicity of metal@TiO_2 to enhance photocatalytic efficiency for CO_2 reduction, ACS Appl. Mater. Interfaces 13 (32) (2021) 38595−38603.
[184] Z.Y. Wang, W. Zhou, X. Wang, X.L. Zhang, H.Y. Chen, H.L. Hu, L.Q. Liu, J.H. Ye, D.F. Wang, Enhanced photocatalytic CO_2 reduction over TiO_2 using metalloporphyrin as the cocatalyst, Catalysts 10 (6) (2020) 654.
[185] Y.L. Zhao, Y.C. Wei, X.X. Wu, H.L. Zheng, Z. Zhao, J. Liu, J.M. Li, Graphene-wrapped Pt/TiO_2 photocatalysts with enhanced photogenerated charges separation and reactant adsorption for high selective photoreduction of CO_2 to CH_4, Appl. Catal., B 226 (2018) 360−372.
[186] J.K. You, M. Xiao, Z.L. Wang, L.Z. Wang, Non-noble metal-based cocatalysts for photocatalytic CO_2 reduction, J. CO_2 Util. 55 (2022) 101817.
[187] J. Ran, M. Jaroniec, S.Z. Qiao, Cocatalysts in semiconductor-based photocatalytic CO_2 reduction: achievements, challenges, and opportunities, Adv. Mater. 30 (7) (2018) 1704649.
[188] J.Y. Zhang, J.J. Xu, F.F. Tao, Interface modification of TiO_2 nanotubes by biomass-derived carbon quantum dots for enhanced photocatalytic reduction of CO_2, ACS Appl. Energy Mater. 4 (11) (2021) 13120−13131.
[189] F.Y. Xu, B.C. Zhu, B. Cheng, J.G. Yu, J.S. Xu, 1D/2D TiO_2/MoS_2 hybrid nanostructures for enhanced photocatalytic CO_2 reduction, Adv. Opt. Mater. 6 (23) (2018) 1800911.
[190] Z. Xiong, Z. Lei, C.C. Kuang, X.X. Chen, B.G. Gong, Y.C. Zhao, J.Y. Zhang, C.G. Zheng, J.C.S. Wu, Selective photocatalytic reduction of CO_2 into CH_4 over Pt-Cu_2O TiO_2 nanocrystals: the interaction between Pt and Cu_2O cocatalysts, Appl. Catal., B 202 (2017) 695−703.
[191] J.J. Dong, Y. Kong, H. Cao, Z.Y. Wang, Z.R. Zhang, L.D. Zhang, S. Sun, C. Gao, X.D. Zhu, J. Bao, Visible-light deposition of CrO cocatalyst on TiO_2: Cr valence regulation for superior photocatalytic CO_2 reduction to CH_4, J. Energy Chem. 64 (2022) 103−112.
[192] J.J. Dong, Z.Y. Wang, H. Cao, J.W. Xue, C.Y. Liu, S. Sun, C. Gao, X.D. Zhu, J. Bao, Independent Cr2O3 functions as efficient cocatalyst on the crystal facets engineered TiO_2 for photocatalytic CO_2 reduction, Appl. Surf. Sci. 554 (2021) 149634.
[193] Y. Zhou, Q. Ye, X. Shi, Q. Zhang, Q. Song, C. Zhou, D. Li, D. Jiang, Ni_3B as p-block element-modulated cocatalyst for efficient photocatalytic CO_2 reduction, Inorg. Chem. 61 (43) (2022) 17268−17277.
[194] Y. Feng, C. Wang, P. Cui, C. Li, B. Zhang, L. Gan, S. Zhang, X. Zhang, X. Zhou, Z. Sun, K. Wang, Y. Duan, H. Li, K. Zhou, H. Huang, A. Li, C. Zhuang, L. Wang, Z. Zhang, X. Han, Ultrahigh photocatalytic CO_2 reduction efficiency and selectivity manipulation by single-tungsten-atom oxide at the atomic step of TiO_2, Adv. Mater. 34 (17) (2022) e2109074.
[195] W. Tu, Y. Li, L. Kuai, Y. Zhou, Q. Xu, H. Li, X. Wang, M. Xiao, Z. Zou, Construction of unique two-dimensional MoS_2-TiO_2 hybrid nanojunctions: MoS_2 as a promising cost-effective cocatalyst toward improved photocatalytic reduction of CO_2 to methanol, Nanoscale 9 (26) (2017) 9065−9070.
[196] Y.M. Yang, M. Liu, S.T. Han, H.L. Xi, C. Xu, R.S. Yuan, J.L. Long, Z.H. Li, Double-sided modification of TiO_2 spherical shell by graphene sheets with enhanced photocatalytic activity for CO_2 reduction, Appl. Surf. Sci. 537 (2021) 147991.
[197] Q.H. Zhang, W.D. Han, Y.J. Hong, J.G. Yu, Photocatalytic reduction of CO_2 with H_2O on Pt-loaded TiO_2 catalyst, Catal. Today 148 (3−4) (2009) 335−340.
[198] Z. Jiang, W. Sun, W. Miao, Z. Yuan, G. Yang, F. Kong, T. Yan, J. Chen, B. Huang, C. An, G.A. Ozin, Living atomically dispersed Cu ultrathin TiO_2 nanosheet CO_2 reduction photocatalyst, Adv. Sci. 6 (2019) 1900289.
[199] Z.L. Wang, J.J. Fan, B. Cheng, J.G. Yu, J.S. Xu, Nickel-based cocatalysts for photocatalysis: hydrogen evolution, overall water splitting and CO_2 reduction, Mater. Today Phys. 15 (2020) 100279.
[200] X.H. Zhang, Z.M. Yuan, J.C. Chen, G.H. Yang, D.D. Dionysiou, B.B. Huang, Z.Y. Jiang, Enhanced CO_2 photoconversion activity of TiO_2 via double effect of CoPi as hole traps and high CO_2 capture, Catal. Today 340 (2020) 204−208.
[201] S. Neatu, J.A. Macia-Agullo, P. Concepcion, H. Garcia, Gold-copper nanoalloys supported on TiO_2 as photocatalysts for CO_2 reduction by water, J. Am. Chem. Soc. 136 (45) (2014) 15969−15976.
[202] D. Tan, J. Zhang, J. Shi, S. Li, B. Zhang, X. Tan, F. Zhang, L. Liu, D. Shao, B. Han, Photocatalytic CO_2 transformation to CH_4 by Ag/Pd bimetals supported on N-doped TiO_2 nanosheet, ACS Appl. Mater. Interfaces 10 (29) (2018) 24516−24522.
[203] Q. Chen, X.J. Chen, M.L. Fang, J.Y. Chen, Y.J. Li, Z.X. Xie, Q. Kuang, L.S. Zheng, Photo-induced Au−Pd alloying at TiO_2 {101} facets enables robust CO_2 photocatalytic reduction into hydrocarbon fuels, J. Mater. Chem. A 7 (3) (2019) 1334−1340.
[204] J. Liu, M. Liu, X.L. Yang, H. Chen, S.F. Liu, J.Q. Yan, Photo-redeposition synthesis of bimetal Pt−Cu co-catalysts for TiO_2 photocatalytic solar-fuel production, ACS Sustain. Chem. Eng. 8 (15) (2020) 6055−6064.
[205] J. Ma, C. Zhou, J. Long, Z. Ding, R. Yuan, C. Xu, Reducing the barrier effect of graphene sheets on a Ag cocatalyst to further improve the photocatalytic performance of TiO_2, RSC Adv. 8 (25) (2018) 14056−14063.
[206] Y. Yu, X. Dong, P. Chen, Q. Geng, H. Wang, J. Li, Y. Zhou, F. Dong, Synergistic effect of Cu single atoms and Au-Cu alloy nanoparticles on TiO_2 for efficient CO_2 photoreduction, ACS Nano 15 (9) (2021) 14453−14464.
[207] Y.C. Wei, X.X. Wu, Y.L. Zhao, L. Wang, Z. Zhao, X.T. Huang, J. Liu, J.M. Li, Efficient photocatalysts of TiO_2 nanocrystals-supported PtRu alloy nanoparticles for CO_2 reduction with H_2O: synergistic effect of Pt-Ru, Appl. Catal., B 236 (2018) 445−457.
[208] J.Q. Gao, Q.Q. Shen, R.F. Guan, J.B. Xue, X.G. Liu, H.S. Jia, Q. Li, Y.C. Wu, Oxygen vacancy self-doped black TiO_2 nanotube arrays by aluminothermic reduction for photocatalytic CO_2 reduction under visible light illumination, J. CO_2 Util. 35 (2020) 205−215.
[209] W. Fang, L. Khrouz, Y. Zhou, B. Shen, C. Dong, M. Xing, S. Mishra, S. Daniele, J. Zhang, Reduced {001}-TiO_{2-x} photocatalysts: noble-metal-free CO_2 photoreduction for selective CH_4 evolution, Phys. Chem. Chem. Phys. 19 (21) (2017) 13875−13881.

[210] W. Zhang, J.B. Xue, Q.Q. Shen, S.F. Jia, J.Q. Gao, X.G. Liu, H.S. Jia, Black single-crystal TiO_2 nanosheet array films with oxygen vacancy on {001} facets for boosting photocatalytic CO_2 reduction, J. Alloys Compd. 870 (2021) 159400.
[211] T. Zhang, J. Low, J. Yu, A.M. Tyryshkin, E. Mikmekova, T. Asefa, A blinking mesoporous TiO_{2-x} composed of nanosized anatase with unusually long-lived trapped charge carriers, Angew. Chem. Int. Ed. 59 (35) (2020) 15000–15007.
[212] H.C. Xi, Y.J. Xu, W.X. Zou, J.W. Ji, Y.D. Cai, H.Q. Wan, L. Dong, Enhanced methanol selectivity of CuO/TiO_2 photocatalytic CO_2 reduction: synergistic mechanism of surface hydroxyl and low-valence copper species, J. CO_2 Util. 55 (2022) 101825.
[213] Z.Q. He, J.T. Tang, J. Shen, J.M. Chen, S. Song, Enhancement of photocatalytic reduction of CO_2 to CH_4 over TiO_2 nanosheets by modifying with sulfuric acid, Appl. Surf. Sci. 364 (2016) 416–427.
[214] X. Qian, W. Yang, S. Gao, J. Xiao, S. Basu, A. Yoshimura, Y. Shi, V. Meunier, Q. Li, Highly selective, defect-Induced photocatalytic CO_2 reduction to acetaldehyde by the Nb-doped TiO_2 nanotube array under simulated solar illumination, ACS Appl. Mater. Interfaces 12 (50) (2020) 55982–55993.
[215] T. Billo, F.Y. Fu, P. Raghunath, I. Shown, W.F. Chen, H.T. Lien, T.H. Shen, J.F. Lee, T.S. Chan, K.Y. Huang, C.I. Wu, M.C. Lin, J.S. Hwang, C.H. Lee, L.C. Chen, K.H. Chen, Ni-nanocluster modified black TiO_2 with dual active sites for selective photocatalytic CO_2 reduction, Small 14 (2) (2018) 1702928.
[216] X. Xin, T. Xu, L. Wang, C. Wang, Ti^{3+}-self doped brookite TiO_2 single-crystalline nanosheets with high solar absorption and excellent photocatalytic CO_2 reduction, Sci. Rep. 6 (2016) 23684.
[217] H.X. Deng, X.T. Zhu, Z.J. Chen, K. Zhao, G. Cheng, Oxygen vacancy engineering of TiO_{2-x} nanostructures for photocatalytic CO_2 reduction, Carbon Lett 32 (7) (2022) 1671–1680.
[218] W. Tu, Y. Zhou, Z. Zou, Photocatalytic conversion of CO_2 into renewable hydrocarbon fuels: state-of-the-art accomplishment, challenges, and prospects, Adv. Mater. 26 (27) (2014) 4607–4626.
[219] V.P. Indrakanti, J.D. Kubicki, H.H. Schobert, Photoinduced activation of CO_2 on Ti-based heterogeneous catalysts: current state, chemical physics-based insights and outlook, Energy Environ. Sci. 2 (7) (2009) 745.
[220] R.F. Chong, Y.Y. Fan, Y.Q. Du, L. Liu, Z.X. Chang, D.L. Li, Hydroxyapatite decorated TiO_2 as efficient photocatalyst for selective reduction of CO_2 with H_2O into CH_4, Int. J. Hydrogen Energy 43 (49) (2018) 22329–22339.
[221] F.Y. Xu, K. Meng, B. Cheng, J.G. Yu, W.K. Ho, Enhanced photocatalytic activity and selectivity for CO_2 reduction over a TiO_2 nanofibre mat using Ag and MgO as Bi-cocatalyst, ChemCatChem 11 (1) (2018) 465–472.
[222] N. Shehzad, M. Tahir, K. Johari, T. Murugesan, M. Hussain, A critical review on TiO_2 based photocatalytic CO_2 reduction system: strategies to improve efficiency, J. CO_2 Util. 26 (2018) 98–122.
[223] D.E. Lee, D.J. Kim, S. Moru, M.G. Kim, W.K. Jo, S. Tonda, Highly-configured TiO_2 hollow spheres adorned with N-doped carbon dots as a high-performance photocatalyst for solar-induced CO_2 reduction to methane, Appl. Surf. Sci. 563 (2021) 150292.
[224] Z.Y. Jiang, X.H. Zhang, Z.M. Yuan, J.C. Chen, B.B. Huang, D.D. Dionysiou, G.H. Yang, Enhanced photocatalytic CO_2 reduction via the synergistic effect between Ag and activated carbon in TiO_2/AC-Ag ternary composite, Chem. Eng. J. 348 (2018) 592–598.
[225] Z.Y. Jiang, W.K. Miao, X.L. Zhu, G.H. Yang, Z.M. Yuan, J.C. Chen, X.X. Ji, F.G. Kong, B.B. Huang, Modifying lewis base on TiO_2 nanosheets for enhancing CO_2 adsorption and the separation of photogenerated charge carriers, Appl. Catal., B 256 (2019) 117881.
[226] D. Wu, J. Guo, H. Wang, X. Zhang, Y. Yang, C. Yang, Z. Gao, Z. Wang, K. Jiang, Green synthesis of boron and nitrogen co-doped TiO_2 with rich B-N motifs as Lewis acid-base couples for the effective artificial CO_2 photoreduction under simulated sunlight, J. Colloid Interface Sci. 585 (2021) 95–107.
[227] Z. Li, C. Mao, Q. Pei, P.N. Duchesne, T. He, M. Xia, J. Wang, L. Wang, R. Song, A.A. Jelle, D.M. Meira, Q. Ge, K.K. Ghuman, L. He, X. Zhang, G.A. Ozin, Engineered disorder in CO_2 photocatalysis, Nat. Commun. 13 (1) (2022) 7205.
[228] J.Y. Ma, Q.Q. Zhang, Z.Y. Chen, K. Kang, L.H. Pan, S.Q. Wu, C. Chen, Z.Q. Wu, J.L. Zhang, L.Z. Wang, Design of frustrated Lewis pair in defective TiO_2 for photocatalytic non-oxidative methane coupling, Chem Catal. 2 (7) (2022) 1775–1792.
[229] T.Z. Li, W.N. Zhang, H. Qin, L. Lu, S.C. Yan, Z.G. Zou, Inorganic frustrated Lewis pairs in photocatalytic CO_2 reduction, ChemPhotoChem 5 (6) (2021) 495–501.
[230] K.K. Ghuman, L.B. Hoch, P. Szymanski, J.Y. Loh, N.P. Kherani, M.A. El-Sayed, G.A. Ozin, C.V. Singh, Photoexcited surface frustrated Lewis pairs for heterogeneous photocatalytic CO_2 reduction, J. Am. Chem. Soc. 138 (4) (2016) 1206–1214.
[231] X.L. Zhu, H.B. Zong, C.J.V. Pérez, H.H. Miao, W. Sun, Z.M. Yuan, S.H. Wang, G.X. Zeng, H. Xu, Z.Y. Jiang, G.A. Ozin, Supercharged CO_2 photothermal catalytic methanation: high conversion, rate, and selectivity, Angew. Chem. Int. Ed. 62 (22) (2023) e202218694.
[232] Y. Yu, X. Dong, P. Chen, Q. Geng, H. Wang, J. Li, Y. Zhou, F. Dong, Synergistic effect of Cu single atoms and Au-Cu alloy nanoparticles on TiO_2 for efficient CO_2 photoreduction, ACS Nano 15 (9) (2021) 14453–14464.
[233] Y.J. Ma, X.X. Yi, S.L. Wang, T. Li, B.E. Tan, C.C. Chen, T. Majima, E.R. Waclawik, H.Y. Zhu, J.Y. Wang, Selective photocatalytic CO_2 reduction in aerobic environment by microporous Pd-porphyrin-based polymers coated hollow TiO_2, Nat. Commun. 13 (1) (2022) 1400.
[234] D. Chen, H. Xing, C. Wang, Z. Su, Highly efficient visible-light-driven CO_2 reduction to formate by a new anthracene-based zirconium MOF via dual catalytic routes, J. Mater. Chem. A 4 (7) (2016) 2657–2662.
[235] L. Zhao, J. Bian, X. Zhang, L. Bai, L. Xu, Y. Qu, Z. Li, Y. Li, L. Jing, Construction of ultrathin S-Scheme heterojunctions of single Ni atom immobilized Ti-MOF and $BiVO_4$ for CO_2 photoconversion of nearly 100% to CO by pure water, Adv. Mater. 34 (41) (2022) 2205303.
[236] J. Bian, J. Feng, Z. Zhang, Z. Li, Y. Zhang, Y. Liu, S. Ali, Y. Qu, L. Bai, J. Xie, D. Tang, X. Li, F. Bai, J. Tang, L. Jing, Dimension-matched zinc phthalocyanine/$BiVO_4$ ultrathin nanocomposites for CO_2 reduction as efficient wide-visible-light-driven photocatalysts via a cascade charge transfer, Angew. Chem. Int. Ed. 58 (32) (2019) 10873–10878.